Hydrol. Earth Syst. Sci. Discuss., 12, 6575–6633, 2015
www.hydrol-earth-syst-sci-discuss.net/12/6575/2015/
doi:10.5194/hessd-12-6575-2015

Hydrology and Earth System Sciences
Open Access
Discussions

# Investigating the impact of land-use land-cover change on Indian summer monsoon daily rainfall and temperature during 1951–2005 using a regional climate model

**S. Halder**[1], **S. K. Saha**[2], **P. A. Dirmeyer**[1], **T. N. Chase**[3], and **B. N. Goswami**[4]

[1]Center for Ocean–Land–Atmosphere Studies, George Mason University, Fairfax 22030, VA, USA
[2]Indian Institute of Tropical Meteorology, Dr. Homi Bhabha Road, Pashan, Pune-411008, India
[3]Cooperative Institute for Research in Environmental Sciences (CIRES), Boulder, CO 80309, USA
[4]Indian Institute of Science Education and Research, Dr. Homi Bhabha Road, Pashan, Pune-411008, India

Received: 27 April 2015 – Accepted: 25 May 2015 – Published: 09 July 2015

Correspondence to: S. Halder (shalder3@gmu.edu)

Published by Copernicus Publications on behalf of the European Geosciences Union.

## Abstract

Daily moderate rainfall events, that constitute a major portion of seasonal summer monsoon rainfall over central India, have decreased significantly during the period 1951 till 2005. Mean and extreme near surface daily temperature during the monsoon season have also increased by a maximum of 1–1.5 °C. Using simulations made with a high-resolution regional climate model (RegCM4) with prescribed vegetation cover of 1950 and 2005, it is demonstrated that part of the above observed changes in moderate rainfall events and temperature have been caused by land-use land-cover change (LULCC) which is mostly anthropogenic. Model simulations show that the increase in seasonal mean and extreme temperature over central India coincides with the region of decreased (increased) forest (crop) cover. The results also show that land-use land-cover alone causes warming in the extremes of daily mean and maximum temperatures by maximum of 1–1.2 °C, that is comparable with the observed increasing trend in the extremes. Decrease (increase) in forest (crop) cover reduces the evapotranspiration over land and large-scale convective instability, apart from decreasing the moisture convergence. These factors act together not only in reducing the moderate rainfall events over central India but also the amount of rainfall in that category, significantly. This is the most interesting result of this study. Additionally, the model simulations are repeated by removing the warming trend in sea surface temperatures. As a result, there is enhanced warming at the surface and decrease in moderate rainfall events over central India. Results from the additional experiments corroborate our initial findings and confirm the contribution of land-use land-cover change on increase in daily mean and extreme temperature and decrease in moderate rainfall events. This study not only demonstrates the important implications of LULCC over India, but also shows the necessity for inclusion of projected anthropogenic changes in land-use land-cover in future climate change scenarios for developing better adaptation and mitigation strategies.

## 1 Introduction

Observational evidences show that globally averaged annual mean surface temperature has increased by about 0.85 °C between 1880 and 2012, with rapid warming in the recent past decades (about 0.72 °C after 1951) (IPCC AR5, Stocker et al., 2014). The IPCC AR5 also summarizes that the number of cold (warm) days and nights have decreased (increased) globally, with increase in the frequency of heat waves over large parts of Europe, Asia and Australia. Apart from surface temperature, extreme (heavy) precipitation events have also increased over most of the global land areas (Alexander et al., 2006; Stocker et al., 2014). The increase in mean precipitation is expected to be much less than the extremes as it is constrained by the net rate of cooling of the troposphere, which, in turn also depends on its temperature and presence of Greenhouse Gases (GHGs) and aerosols (Allen and Ingram, 2002). The IPCC AR5 summarizes that there is *medium confidence* on the contribution of human influence on large-scale changes in land precipitation. Furthermore, Seneviratne et al. (2012) argues that there is no general relationship between changes in total and extreme precipitation. However, seasonal and regional or local changes in these extremes can be of different magnitude and sign due to complex regional feedbacks associated with the GHGs, clouds, aerosols and other anthropogenic activities. Haerter and Berg (2009) argue that changes in humidity, atmospheric stability, wind direction etc. strongly influence the local temperature variability. Observational uncertainty, challenges in modeling and natural variability affect proper detection and attribution of the changes. Therefore, quantification of the changes in regional climate and proper attribution are both very important for the policy makers for devising better adaptation and mitigation strategies.

Studies on trends in extreme temperature and precipitation events over the Indian sub-continent have focused on different regions and periods. Kothawale et al. (2010, 2005) found an overall increase of about 0.5 °C (0.71 °C) in the annual mean (maximum) temperature over seven homogeneous regions of India in the last century.

They also reported an accelerated warming trend of 0.22 °C decade$^{-1}$ in the mean annual temperature in the recent decades (1971–2003). Jaswal et al. (2015) using station observations reported a significant increase in high temperature in summer over India during the period 1969–2013. Pai et al. (2013) also reported a significant increase in occurrence of heat waves in summer during 1961–2010. Sheikh et al. (2014), using daily station data found a general increase in warm temperature (precipitation) extremes during 1971–2000 (1961–2000), with enhanced warming over the desert of Thar. They associated those changes with the effect of increasing aerosols. Over central India (CI, 74.5–86.5° E; 16.5–26.5° N), heavy and very heavy (moderate) rainfall events during the monsoon season (June–September, JJAS) have been reported to show a significant increasing (decreasing) trend from 1951 to 2000 (Goswami et al., 2006). Rajeevan et al. (2008) and Pai and Sridhar (2015) supported that result and reported a similar but relatively weaker trend in heavy and moderate rainfall events over that region from 1901 to 2000. Singh et al. (2014) reported a significant decrease in monsoon precipitation over that core (CI) region of India from 1951 till 2011, along with a significant increase in frequency of dry spells and intensity of wet spells and decrease in intensity of dry spells. Niranjan Kumar et al. (2013) found an increase in the intensity of droughts during 1901 till 2010 over India. Panda et al. (2014) reported a significant decrease in wet days and moderate and total rainfall during the summer monsoon (1971–2005) over the northeast, central and southwest of India. Both studies attributed their observed trends with evolving SST anomalies over the Pacific and Indian Oceans. Although Goswami et al. (2006) and Rajeevan et al. (2008) pointed at warming of the Indian Ocean sea surface temperature (SST) to be the governing factor for increase in precipitation extremes, the probable reason for decrease in moderate rainfall events was left unaddressed. Observed changes in daily high temperature and moderate/extreme rainfall events over the Indian region may be attributed to both natural variability and anthropogenic activity. Extreme high or low temperature phases are not only harmful for crop growth and yield but heat/cold waves and heavy rainfall events also cause fatality of living beings. Light to moderate rainfall events constitute a major portion of the seasonal rainfall over India and are an important source for replenishment of ground water. The aim of this study is to understand the processes responsible for observed changes in moderate rainfall events and daily mean and maximum temperature over India during the monsoon season.

### 1.1 Role of land use/land cover change in climate

Land use/land cover change (LULCC) is an important driver of climate change at local, regional and possibly, also on global scale (Snyder, 2010) and on time scales inter-decadal and beyond (Pitman et al., 2012; Mahmood et al., 2014; Dirmeyer et al., 2010; Solomon et al., 2007). LULCC affects the surface albedo, fluxes of radiation and that of momentum, heat, water vapor, carbon dioxide ($CO_2$) and other trace gases, aerosols and dust, and turbulence in the boundary layer (Pielke et al., 2011; Mahmood et al., 2014). In the last 300 years (1700–2000), about 42–68 % of the global land surface has been affected due to land use practices (Hurtt et al., 2006). There has been an increase in global cropland (Ramankutty et al., 1999, 2008) and pastures (Goldewijk et al., 2001). For a concise summary of the evolution of LULCC across centuries, refer Fig. 1 of the paper by Pielke et al. (2011) that is based on the Land Use Harmonization data (http://luh.unh.edu). Cropland areas and pastures in general, decrease the surface temperature on account of their higher albedo than forests. Likewise, irrigated agricultural landscapes also contribute to surface cooling and rainfall (Pielke et al., 2011; Mahmood et al., 2014). However, the effects of deforestation and agricultural intensification vary regionally and also depend on the seasons, making resulting land–atmosphere interactions complex. Robust results show that albedo changes leading to decrease in surface temperature tend to dominate over the mid-latitudes, whereas decrease in evapotranspiration (ET) and roughness length play a primary role in increasing surface warming in the Tropics (Garratt, 1993; Sampaio et al., 2007; Davin and De Noblet-Ducoudr‘e, 2010; Pitman et al., 2012). The above conclusions are supported in studies by Lawrence and Chase (2010), Bounoua et al. (2002) and Feddema et al. (2005). Deforestation and increases in crop cover reduces the surface roughness and also decreases the moisture convergence and rainfall (Sud et al., 1998). Spatial heterogeneity in vegetation has been shown to affect convective rainfall through changes in surface fluxes of heat and moisture and atmospheric stability (Pielke et al., 2001). Lawrence and Chase (2010) further demonstrated that alteration of potential vegetation to present day land cover state can lead to regional warming as well as reduction in precipitation. In an interesting study, Avila et al. (2012) demonstrated that changes in the temperature extremes due to LULCC could be of comparable magnitude but of similar or opposite sign as due to increase in $CO_2$, depending on the region. Pitman et al. (2012) supported those conclusions using a multi-model ensemble study, and also extended their analysis for rainfall extremes. Since it is difficult to segregate the impact of LULCC on temperature and precipitation extremes when analyzed in a globally averaged sense (Pielke et al., 2011; Pitman et al., 2012), one needs to carefully design sensitivity studies with climate models and focus on specific regions to better understand its role.

## 1.2 LULCC in the context of India

Over India, industrialization and urbanization has grown immensely from the middle of the 20th century, apart from the Green revolution. This has lead to widespread deforestation and changes in land-use practices towards agriculture. A recent study over India by Tian et al. (2014) using high-resolution remote sensing datasets from the Resourcesat-1 satellite and historical archives at district and state level show loss (gain) of about 26 (48.1) million ha of forests (crops) over the period 1880–2010. Greater cropland expansion and urbanization occurred during 1950–1980 but mostly over central, eastern and northwest India and eastern and western parts of peninsular India (refer Fig. 4 in their paper). Such regional changes in LULC could have caused changes in the Indian climate through their impact on the surface moisture and heat budget, and may have amplified or compensated other potential changes due to increased GHGs, aerosols, large-scale circulation changes or natural variability. Therefore, it is important to quantify whether the decrease in moderate rainfall events over CI and how much of the observed changes in daily mean and extreme surface temperature over India in the later half of the 20th century is attributed to LULCC?

As mentioned earlier, the increasing trend in heavy rainfall events over CI has been potentially associated with a significant increasing trend in SST over the tropical Indian Ocean (Goswami et al., 2006; Rajeevan et al., 2008) that has been also reported in Roxy et al. (2014). Sen Roy et al. (2007, 2011) found a significant decrease (increase) in pre-monsoon (March–May) surface temperature (precipitation) over India due to irrigation activity. Lee et al. (2009) showed that pre-monsoon irrigation activity could affect the early part of the Indian Summer Monsoon Rainfall (ISMR) through changes in land-ocean temperature contrast. Niyogi et al. (2010) found an overall decrease in rainfall during monsoon season over the northwest of India due to irrigation and land-use change. Similarly, Tuinenburg et al. (2011) used model simulations to conclude that large-scale irrigation might increase local precipitation over eastern and southern India through land–atmosphere feedbacks. Nayak and Mandal (2012) used model studies to attribute increased warming over western India (1973–2009) to LULCC. There have been similar other studies as well like Lohar and Pal (1995), Douglas et al. (2006), Saeed et al. (2009), Dutta et al. (2009). Kishtawal et al. (2010) reported an influence of growing urbanization on the increasing trend of extreme rainfall events over India. Ali et al. (2014), on the contrary, found large-scale climate variability and not urbanization in India responsible for observed changes in extreme rainfall events. LULCC not only involves an increase in irrigated lands but also deforestation, afforestation, conversion to bare, pasture or cropland and urbanization as well. Global model simulations by Takata et al. (2009) using historical reconstructed LULC (years 1700 and 1850 during the pre-industrial period) showed a weakening of the Indian summer monsoon circulation and a decrease in seasonal rainfall due to an increase in crop and pasture land. Earlier studies have not focused on the changes in the frequency and intensity of daily rainfall or temperature extremes. Likewise, the mechanism for decrease in light and moderate rainfall events is not understood and has also not been investigated. In this study, we demonstrate that LULCC over India has contributed partly to the observed decrease in moderate rainfall events during the monsoon season from 1951 till 2005. Apart from that, we also show that LULCC has contributed to the significant increasing trend in surface daily mean and maximum temperatures during summer season. For that purpose, we have used high resolution improved and up-to-date LULC data over the Indian region.

High-resolution regional climate model (RCM) simulations with RegCM4 have been made to support our hypothesis. RCMs have shown improvements over global models in terms of representation of spatio-temporal details of climate (Laprise et al., 2008; Leduc and Laprise, 2009) and in dynamical downscaling ability (Xue et al., 2014). RCMs add value in simulation of topography induced phenomena and extremes of short spatio-temporal character (Feser et al., 2011; Feser and Barcikowska, 2012; Shkol'nik et al., 2012). They have also shown improvement in representation of large-scale monsoon features over East Asia (Gao et al., 2012). The main advantage of a RCM in the context of the Indian monsoon is that it can isolate external forcing generated in remote areas by the local feedback processes within the monsoon region or else, they may interact with the internal monsoon dynamics and produce more variability. In that way, a RCM better resolves regional land–atmosphere feedback processes than a GCM. However, one of the disadvantages is that the lateral boundary conditions may not be perfect. Studies by Saha et al. (2011, 2012) have demonstrated the capability of the RCM RegCM3 (previous version of RegCM4) in simulating the mean and interannual variability of the Indian summer monsoon.

This paper is organized as follows. Observed data, the RCM and the design of experiments are described in detail Sect. 2. Method of preparation of the LULC data used for model experiments is described in the Supplement. Herein, a brief description about preparation of the LULC data that is used in model simulations is also presented. The observed changes in near surface temperature and rainfall and LULC over the Indian subcontinent in the last 55 years are discussed in Sect. 3. Results from model experiments pertaining to changes in rainfall and surface temperature are discussed in

Title Page
Abstract Introduction
Conclusions References
Tables Figures
◀◀ ▶▶
◀ ▶
Back Close
Full Screen / Esc
Printer-friendly Version
Interactive Discussion

detail in Sect. 4. Discussions are presented in Sect. 5 and the conclusions drawn are summarized in Sect. 6.

## 2 Data and methods

### 2.1 Observed data

Daily 2 m mean and maximum temperature data (1969–2005, at 1° × 1° resolution) from the India Meteorological Department (IMD) (Srivastava et al., 2009) are used for analysis of trends and validation of the model simulations. In addition to that, we have also used daily 2 m mean temperature data (at 2.0° × 2.0° resolution) of the twentieth century reanalysis (20CR) project (Compo et al., 2011) that is available for a longer period (1951–2005). For analysis of trends in daily rainfall events and their intensities in different categories daily gridded data (at 1° × 1° resolution) for 57 years (1951–2007) from IMD (Rajeevan et al., 2006) is used. These observed data available from IMD are one of the most reliable data sets at high resolution (http://www.imdpune.gov.in/publication/pub_index.html). Monthly rainfall from GPCP version 2.2 (Adler et al., 2003) for the period 1979 to 2008 (at 2.5° × 2.5° resolution) is also used for validation of model simulated rainfall. Apart from that, the National Centers for Environmental Prediction/National Center for Atmospheric Research (NCEP/NCAR) monthly reanalysis winds, temperature and specific humidity (Kalnay et al., 1996) for the period 1982–2008, at 2.5° × 2.5° horizontal resolution and multiple pressure levels are used for validation of the model simulated large-scale features during monsoon.

### 2.2 LULC data

Annual harmonized LULCC data (LUHa.v1) from the University of New Hampshire (UNH, http://luh.unh.edu) at 0.5° × 0.5° horizontal resolution (Hurtt et al., 2006) that comprises of crop, pasture and primary and secondary vegetation types has been used. This data has been transformed in the form of 17 Plant Functional Type (PFT) mosaics for use as time invariant lower boundary condition for RCM simulations coupled with the Community Land Model (CLM) land surface model in this study. The four UNH vegetation categories are converted into different CLM PFT distributions based on present day and potential vegetation CLM land surface parameters. We have used the resulting PFT distributions and associated vegetation dependent parameters such as LAI, Stem Area Index (SAI), roughness length etc. for the present day conditions (year 2005) and historical period (year 1950) for our model simulations. Detailed methodology of preparation of the LULC data is given in the Supplement.

### 2.3 RegCM4.0 and the CLM3.5 land surface model

The RCM RegCM version4.0 (Elguindi et al., 2010; Giorgi et al., 2012) is used for this study. The dynamical core of RegCM4 is from the NCAR-Pennsylvania State University (PSU) Mesoscale Model version 4 (MM4), which is a compressible, finite difference model with hydrostatic balance and vertical $\sigma$-coordinates. The NCAR CCM3 radiation scheme (Kiehl et al., 1996) and a planetary boundary layer scheme based on a non-local diffusion concept (Holtslag et al., 1999) are used for our simulations. We also used the new parameterization scheme of Zeng et al. (2005) that allows for a realistic representation of the diurnal variation sea surface skin temperature. Apart from that, the Grell convective parameterization scheme (Grell, 1993) with the Fritsch and Chappell closure (Fritsch and Chappel, 1980) is used. The model configuration comprises of 23 vertical sigma coordinate levels in the atmosphere and a horizontal resolution of $60^\circ \times 60^\circ$ km with Normal Mercator map projection. The model domain extends from 40.2–116.3° E and 10.8° S–47.7° N with the Indian subcontinent at the center. Recent studies with a similar model configuration as this (Saha et al., 2011, 2012) has demonstrated fidelity of the RCM in simulating the climatological features of Indian summer monsoon. The NCEP/NCAR reanalysis data (Kalnay et al., 1996) at $2.5^\circ \times 2.5^\circ$ horizontal resolution and 6 hourly frequency for the period 1982 to 2008 is used as lateral boundary conditions for the model. Reynolds weekly SST at $1^\circ \times 1^\circ$

horizontal resolution (Reynolds et al., 2002) interpolated to daily values is prescribed over the ocean.

RegCM4.0 is coupled to the Community Land Model (CLMv3.5) (Oleson et al., 2008; Stockli et al., 2008) land surface model. There are 10 soil layers of variable depth and up to 5 layers of snow. CLM3.5 uses a nested sub-grid hierarchy of mosaics in the form of glaciers, lakes, wetlands, urban and vegetated land to better represent surface heterogeneity in a grid box. The vegetated land portion of a grid cell may be composed of multiple columns. Furthermore, in each column 4 most abundant PFTs out of possible 17 that include forests, grasses, crops and bare ground co-exist. The fractional areas of the 4 PFTs do not vary with time but their monthly LAI and stem area index (SAI) values vary seasonally, which are all interpolated from global datasets at $0.5^\circ \times 0.5^\circ$ horizontal resolution to the model grid. Fluxes are computed at the PFT level and their weighted averages constitute the net upward flux from a column. Several PFT based parameters are also prescribed in the model. A global soil texture dataset at 5 min spatial resolution from the International Geosphere Biosphere Program (IGBP) (Bonan et al., 2002) is used with varying sand and clay content in each of the 10 layers. Soil color dataset (8 classes) at $2.8^\circ$ spatial resolution is from Zeng et al. (2002). CLM3.5 also uses global datasets on canopy top and bottom height (resolution $0.5^\circ \times 0.5^\circ$), percentage of glacier (resolution $0.5^\circ \times 0.5^\circ$), lake and wetland (resolution $1^\circ \times 1^\circ$) with corresponding spatial resolution included in brackets (Elguindi et al., 2010). Details about the land surface parameterization schemes in CLM3.5 are also presented in Oleson et al. (2010) and Tawfik and Steiner (2011).

### 2.4 Design of experiments and methodology

Two sets of model simulation, each for 27 years are carried out with similar Lateral Boundary Conditions (LBCs) from NCEP/NCAR and Reynolds weekly SST prescribed at the lower boundary, but different LULC of the years 1950 and 2005 as fixed lower boundary condition. The LULC of 1950 and 2005 correspond to different PFT distributions. The RCM is initialized at 00:00 GMT on 1 November 1981 and simulation is continued up to 18:00 GMT on 31 December 2008. In CLM3.5 coupled to RegCM4, soil moisture is initialized based on climatology (as in Tawfik and Steiner, 2011; Giorgi and Bates, 1989), in order to reduce model spin-up time for deeper layers. Soil points are initialized with temperatures of 283 K (Oleson et al., 2010). Hereafter, these simulations with LULC of 2005 and 1950 will be referred as Present Land Cover (PLC) and Historical Land Cover (HLC) experiment, respectively. No added external forcing in terms of aerosols or GHG concentration is used in our RCM experiments. Although, our RCM simulations are not time-slice experiments in the true sense, the statistics of their difference are expected to reveal the effect of LULCC and associated regional land–atmosphere interactions on daily temperature and rainfall variability in a climatological sense. Kothawale et al. (2010) and Chowdary et al. (2013) have shown surface temperatures over India and the Indian Ocean SSTs to be strongly linked on low-frequency interannual time scales. Apart from that, Goswami et al. (2006) and Rajeevan et al. (2008) speculated that the increasing trend of extreme rainfall events might be associated with the warming trend in SST over the Indian Ocean. Therefore, in order to isolate the effect of Indian Ocean SSTs on the temperature and rainfall variability over the monsoon region, another two sets of model simulation for 27 years are carried out using the fixed LULC of years 1950 and 2005, but with de-trended weekly Reynolds SSTs over the Indian Ocean. The de-trended weekly SSTs from November 1981 till December 2008 are interpolated to daily values for model simulation. The LBCs from NCEP/NCAR reanalysis and the initial conditions for land remained exactly same as in the earlier experiments. Henceforth, these RCM simulations will be referred as Present Land Cover de-trended SST experiment (PLCS) and Historical Land Cover de-trended SST experiment (HLCS), respectively. The four experiments are briefly summarized in Table 1.

Observed changes in LULC used as fixed boundary condition in the RCM are described in Sect. 3, which also includes discussion on observed changes in surface temperature and daily rainfall distribution during 1951 to 2005. Simulation of the large-scale climatological features of Indian summer monsoon by the RCM in the PLC and

PLCS experiments are discussed in the following Sect. 4.1. Differences in simulated rainfall statistics between experiments with past (1950) and present land cover (2005) are discussed in Sect. 4.2. Of particular importance is our discussion on changes in moderate rainfall events (Sect. 4.2.1). Extreme rainfall events are less frequent but intense, with long return periods. They are associated with deep convective activity that is triggered by local instabilities or large-scale moisture convergence and drain out the atmospheric moisture content very fast, thus increasing the atmospheric stability. On the other hand, light and moderate rainfall events are relatively less intense and long-lived and require time for large-scale moisture and instability to build up for them to sustain. Thus, due to the smaller spatial scale and random frequency of occurrence of extreme rainfall events, analysis of their trends over stations sparsely spaced or individual grid points is not expected to give a robust or consistent result about their temporal variability. Therefore, more meaningful information on the statistics of extreme rainfall events can be obtained when analyzed in a spatially aggregated sense (Goswami et al., 2006; Rajeevan et al., 2008). This approach has also been followed by Singh et al. (2014). For our study, CI domain that is considered homogeneous in terms of the mean and variability of the Indian summer monsoon rainfall (Goswami et al., 2006) is used for the analysis of moderate and extreme rainfall events. Significance of the results have been tested on the basis of Student's *t* test. The effect of LULCC on surface air temperature extremes over India in the experiments with realistic prescribed SSTs and the experiments with de-trended SSTs are discussed in Sect. 4.3. For the analysis on temperature extremes in the model we have used data for the period JJAS (instead of JAS used for observation) that will be discussed in Sect. 4.1. Based on the experiments and further analysis, we propose a physical mechanism responsible for the observed changes in Sect. 4.4.

# 3 Observed changes

## 3.1 LULCC

Figure 1 shows the distribution of PFTs of all forests and crops (including grasses) in the year 1950 and 2005 used as lower boundary condition in the RCM and also gives an overview of past changes in land cover. The northwest of India, the hilly terrain over CI, western states of Gujarat and Maharashtra, foothills of the Himalayas and northeastern states are mostly dominated by forest cover (Fig. 1a and c). Agriculture or crop cover is mostly concentrated along the northern states of India such as Punjab, Haryana, Delhi, the Gangetic plains, the plains of east and west CI and peninsular India (Fig. 1b and d). Difference between PFT distribution under present climatic condition (year 2005) and historical period (year 1950) show that forest cover is reduced and crop cover is increased in the recent period by about 5–30 % (Fig. 1e and f). Maximum increase in crop fraction is seen largely over CI, peninsular India, north and northwest India and extreme northern part around the plains of river Indus. This increase in crop fraction also matches very well with the changes shown in Fig. 5 in the paper by Tian et al. (2014) over the period from 1950 to 2010. Observed surface evaporation has significantly decreased over continental India during the monsoon season from 1971 to 2000 (Jaswal et al., 2008) and may have been associated with the changes in LULC.

## 3.2 Rainfall over central India

There is no clear trend in the all India mean summer monsoon rainfall during JJAS from 1951 till 2000, but extreme and moderate rainfall events have changed over CI significantly (Goswami et al., 2006; Rajeevan et al., 2008). While moderate rainfall events ($5 > \text{rainfall} \le 100\,\text{mm}\,\text{day}^{-1}$) show a significant decreasing trend, the heavy ($\text{rainfall} \ge 100\,\text{mm}\,\text{day}^{-1}$) and very heavy rainfall ($\text{rainfall} > 150\,\text{mm}\,\text{day}^{-1}$) events show a significant increasing trend. As mentioned earlier, increase in heavy and very heavy rainfall events over CI have been potentially associated with a significant increasing trend in SST over the Indian Ocean. However, the physical mechanism for decrease in moderate rainfall events over CI is unknown and is investigated in this study. After counting daily rainfall at each grid point (1° × 1°) over CI as an event, we find that the number of moderate rainfall events between 1951 and 2005 have significantly decreased by about 520, (which is about 10 % of the initial value in 1951), (Fig. 2a). Associated with that, the total rainfall in moderate category has also decreased during JJAS (Fig. 2b). On the contrary, number of extreme rainfall events over CI has significantly increased by about 10 (almost double the value in 1951) between 1951 and 2005 (figure not shown). On the basis of earlier modeling studies that addressed the impact of vegetation cover on rainfall and observed changes in vegetation over India we propose that, LULCC might have contributed to the observed decrease in moderate rainfall over CI. We substantiate our hypothesis using multiple simulations with the RCM RegCM4.

### 3.3 Surface air temperature

The pre-monsoon season in India (March–April–May) is characterized by days that are hot and dry. The climatological onset date of the southwest monsoon over Kerala (southern tip of India) is 1 June. There is large year-to-year variability in the date of onset and in many years, onset takes place during the middle of June (Wang et al., 2009). Therefore, to investigate the changes in observed daily mean temperature and its extreme during the monsoon season, trends are calculated using temperature of the months July–September (JAS) only. A warming trend in the JAS mean temperature by 0.2–0.4 °C decade$^{-1}$ is observed over the northwest, northeast and southern parts of India (Fig. 3a). Similar to the mean, extreme of daily mean temperature in JAS (its 90th percentile) also shows a warming trend, but over a larger region (Fig. 3b). Based on this trend from 1969 till 2005, the daily mean surface temperature and its extreme in JAS have increased by a maximum amount of about 1.11–1.48 °C. Daily maximum temperature represents the maximum temperature attained during the day. Figure 3c shows the trend in JAS averaged daily maximum temperature. It is evident that warming in the daily maximum temperature is of the same order, but is more widespread as compared to the daily mean and includes areas north of CI. Furthermore, 90th percentile of daily maximum temperature has increased by more than 1.48 °C over north-central India, which is greater than increase in the mean (Fig. 3d). It may be noted that the spatial pattern of increase in daily temperature over CI is consistent with the area of increase in crop PFTs over CI and northwest (Fig. 1f). Similarly, the decreasing trend in daily temperature over areas south of CI also coincides well with the small increase in forest cover over that region (Fig. 1e). Increased observed temperature over the western coast of peninsular India may have happened due to its region specific mean climate that is predominantly determined by the adjoining Arabian Sea and Indian Ocean.

We also analyzed the trend in daily 20CR 2 m mean temperature data and its extreme (90th percentile) during JAS for the period 1950–2005. A significantly increasing trend is evident both in the mean and its extreme, over northern India (Fig. 3e), north of CI (Fig. 3f) and southern parts of peninsular India. The maximum increase in daily mean temperature in JAS is about 1.11 °C. The pattern of increase in daily maximum temperature is not only more widespread (possibly due to coarser resolution of the model) but its magnitude is also comparable to that seen over the 37-year period (1969–2005). Apart from that, a decrease south of CI and an increase towards the extreme south is also evident. However, while comparing the trends shown by the above two datasets we note that the model used to generate the 20CR data did not assimilate surface temperature observations. Therefore the resulting trend is also partially model dependent. Observed increasing trend in daily mean surface temperature and its higher extreme may be attributed to forcing of natural (solar, volcanic) or anthropogenic origin (GHGs, aerosols etc.) or both. We aim to quantify the contribution to such increase due to LULCC over India.

## 4 Results from RCM experiments

In the PLC and HLC experiments, we keep the atmospheric and oceanic boundary conditions during 1982 to 2008 similar but the distribution of PFTs are altered corresponding to years 2005 and 1950 respectively. This experimental set-up is meant to help us understand the statistics of changes in rainfall and temperature due to LULCC.

### 4.1 Indian summer monsoon features in PLC and PLCS experiment

The Indian summer monsoon is a large-scale phenomenon and an important driver of boreal climate in the tropics as well as extra-tropics. The skill of the RCM in capturing the mean spatial distribution of seasonal (JJAS) rainfall and its interannual variability are assessed here. The observed seasonal mean monsoon rainfall in GPCP (Fig. 4a) shows a region of maxima over the Western Ghats, head Bay of Bengal (BoB), hilly terrain of Central India and north-east India. There is also a region of maximum over east equatorial Indian Ocean. In comparison, rainfall in the PLC experiment is overestimated near the Arabian Sea coast and over BoB. Apart from that, a secondary rainfall maximum exists which is shifted to the west equatorial Indian Ocean region is also noted in PLC. Although rainfall is also captured over CI and the northeast, the magnitude seems to be underestimated, particularly over western India. Earlier studies have shown that rainfall bias in RCMs over ocean is attributed to the lack of coupling with the atmosphere and also to the choice of convective parameterization schemes (Chow et al., 2006; Ratnam et al., 2009; Saha et al., 2011). However, it is interesting to note that compared to an earlier version of the RCM (RegCM3) used for simulation of the Indian summer monsoon with a similar model set-up (Saha et al., 2011, 2012), this positive bias over the west-equatorial Indian Ocean region and western part of BoB is relatively reduced. The rain-shadow area over peninsular India is captured by the RCM. The dashed (solid) lines in Fig. 4b represent the CI (big-India, BI) domain used for our analysis related distribution of daily rainfall. Seasonal mean rainfall in

PLCS experiment follows a similar spatial pattern as in PLC and captures the locations of rainfall maxima (Fig. 4c). However, the magnitude is relatively less everywhere compared to PLC. Maximum decrease in seasonal total rainfall over CI between PLCS and PLC experiments is about 4 cm (figure not shown). This decrease is possibly due to relatively colder SSTs over the Indian Ocean that leads lesser evaporation over ocean and hence moisture convergence over land. These aspects will be discussed further in Sect. 4.2.

Seasonal rainfall over the land part in PLC (Fig. 4e) is compared with that from IMD and APHRODITE data (Fig. 4c and d). On closer examination it is revealed that the RCM reproduces the regions of rainfall maxima and the spatial pattern reasonably well. However, it seems to slightly underestimate the magnitude of rainfall over peninsular and western part of India. The pattern correlation between rainfall in PLC experiment and APHRODITE is 0.71. The Mean Bias calculated over the presented domain with respect to APHRODITE rainfall for the period 1982–2007 is $-0.48\,\mathrm{mm\,day^{-1}}$ and the RMSE is $3.53\,\mathrm{mm\,day^{-1}}$. Although there are more station observations aggregated into the IMD data, the APHRODITE dataset has also been chosen for its greater spatial extent over land part compared to IMD. Although daily CI averaged rainfall during JJAS in both observation (IMD) and the PLC experiment (CI domain for the RCM is 75.30–86.63° E, 16.92–26.43° N) follows the Poisson distribution, the number of very heavy rainfall events in the RCM is relatively less (figure not shown). This deficiency in climate models in terms of capturing the observed frequency distribution of daily rainfall realistically is a well-known problem (Frei et al., 2003; Kang et al., 2014) and may be attributed to the model dynamics, choice of convective parameterization schemes and their interplay (Frei et al., 2003). The mean and interannual standard deviation of CI averaged rainfall (1982–2007) in PLC (IMD) are 77.59 cm (87.28 cm) and 7.57 cm (8.8 cm), respectively. The model performs reasonably well in capturing the observed interannual variability of seasonal rainfall over CI (which is about 10 % of the seasonal mean), although it underestimates both quantities.

Title Page
Abstract | Introduction
Conclusions | References
Tables | Figures
◄◄ | ►►
◄ | ►
Back | Close
Full Screen / Esc
Printer-friendly Version
Interactive Discussion

Air temperature at 2 m has been used in modeling studies to validate simulated features of the Indian summer monsoon by the RCM (Pal et al., 2007; Saha et al., 2011). JJAS averaged 2 m near-surface air temperature simulated by the model is compared here with the IMD data for the period 1982 till 2005. Mean surface temperature in observation in highest over the north, east, north-west and the rain-shadow region to the east of peninsular India (Fig. S1a in the Supplement). In the model, surface temperature is high particularly over the north-west (Fig. S1b). As a result, a cold bias of about 3–4 °C is found over northern, western and eastern India that is probably linked with the land-surface and other parameterization schemes in the model such as radiation, convection etc. (Fig. S1c). Bias is much higher over extreme north and north-east India. The pattern correlation between IMD and RegCM4 JJAS 2 m air temperature is 0.76. A similar pattern of cold bias in 2 m near surface air temperature is also seen in PLCS experiment (figure not shown). As our objective is to analyze the mean differences between model simulations, these biases are not expected to have significant effect on the results.

Observed large-scale circulation features from NCEP/NCAR reanalysis in the lower troposphere (850 hPa) shows the location of the low-level Somali Jet over the Arabian Sea, cross-equatorial flow and the easterlies south of the Equator (Supplement Fig. S2a). The RCM captures the location of these large-scale low-level features reasonably well in both PLC and PLCS (Fig. S2b and c). However, the wind speed is slightly overestimated in PLC experiment, particularly along the core of the Somali Jet and the BoB. This overestimation conforms to the positive rainfall bias over the Ocean, the Arabian Sea and the BoB in the RCM. Increased precipitation in the model leads to greater release of latent heat in the atmosphere. As circulation and precipitation are convectively coupled, this heating invigorates convection and vertical motion in the atmosphere, which further increases large-scale low-level convergence and hence the strength of circulation. On the contrary, low-level wind speed is reduced around the core of the Jet, over the Indian Ocean, BoB and also over land in the PLCS experiment, which is associated with the reduction in precipitation.

At the upper level (200 hPa) large-scale circulation in observations show the sub-Tropical Westerly Jet stream about north of 30° N, the Tropical Easterly Jet over the equatorial Indian Ocean and the Tibetan Anticyclone south of 30° N (Fig. S2d). Location of these characteristic circulation features is also well captured in the simulations PLC and PLCS (Fig. S2e and f). The model simulated wind speed is stronger than observations in the PLC experiment at upper level like at 850 hPa. The pattern correlation between NCEP/NCAR reanalysis and PLC simulated wind at 850 hPa (200 hPa) is 0.81 (0.95).

The climatological onset date of Indian summer monsoon rainfall (ISMR) based on the Tropospheric Temperature Gradient (TTG) index (Xavier et al., 2007) in the PLC experiment is around 20 May, with interannual standard deviation of about 8 days. Hence, it is advanced by about 10 days from the observed onset. Unlike in the observations, ISMR onset in the model happens to be in the month of May for most years. Therefore, for our analysis of temperature extremes in the model we have used data for the period JJAS (instead of JAS) in order have a longer time series and more confidence in the model results. We infer that the model RegCM4 performs reasonably well in simulating the climatological mean features of Indian summer monsoon. This gives us confidence to conduct sensitivity experiments with the model.

### 4.2 Changes in circulation and seasonal rainfall due to LULCC

Mean surface winds (at 10 m) during JJAS blow from west to east over peninsular India and the Indian Ocean, carrying moisture from the Arabian Sea. They turn anti-clockwise over the BOB to move north-west over the Gangetic plains, thus forming the monsoon trough all along CI where the wind speed is very low (Fig. 5a). As forest cover in HLC experiment is replaced by crop PFTs over most of the land part in PLC experiment, surface roughness length is decreased due to reduction in vegetation height and LAI. We note that surface wind has become more westerly (easterly) over southern and western (northern) India and shows increased anti-cyclonic circulation (Fig. 5b). It has intensified significantly by about 1 m s$^{-1}$ over peninsular India and

$0.5\,\mathrm{m\,s^{-1}}$ over the northern India (Fig. 5c). This implies less convergence of moisture and also a reduction in rainfall in the PLC experiment (see Sud et al., 1998; Takata et al., 2009) to be discussed in the following paragraph. This intensification of surface wind speed further extends up to the depth of the boundary layer that interacts more directly with the large-scale circulation (figure not shown). Surface and boundary layer winds also intensify in a similar fashion in the PLCS experiment when compared to HLCS and depict the effect of reduced roughness length. It is interesting to note that these significant changes take place only over the land portion of the domain and partly over water bodies close to its boundaries.

The climatological seasonal (JJAS) distribution of rainfall over the Indian subcontinent has been discussed in detail in Fig. 4. Difference in seasonal rainfall between PLC and HLC shows a significant reduction over a large part of CI, peninsular and northwest India (Fig. 6a). It is interesting to note that the pattern of decrease matches very well with the regions that show an increase in crop PFTs from 1950 to 2005, with maximum changes over the northwest of India. The magnitude of decrease in seasonal rainfall is quite high (by 5–7 cm) over certain regions, however it is difficult to find out exact reason for such changes at every grid. It may be due to changes in local instability brought about by land–atmosphere feedback processes or changes in large-scale moisture convergence or both. A part of these changes also depend on the choice of parameterization schemes in the RCM. Observational evidence suggests that despite increase in water holding capacity of the atmosphere on a large scale, changes in rainfall are very localized. It is plausible that large-scale conditions and moisture convergence in the PLC experiment might be relatively unfavorable for formation of rainfall compared to the HLC experiment. In order to find out changes in the large-scale moisture convergence, we first calculated vertically integrated moisture flux ($q\boldsymbol{V}$) from surface to 300 hPa. Following Helmholtz's theorem and the methodology of Behera et al. (1999), velocity potential is further calculated that represents the divergent component of that moisture flux. It turns out, from the difference of that divergent component, that large-scale moisture convergence is reduced in the PLC experiment and contributes to the reduction in rainfall over CI (Fig. 6a). However, it also remains to be explored how much do the changes in LULC contributes to reduction in surface evaporation and hence moisture convergence over land. This will be discussed in Sects. 4.3 and 4.4. It is known from earlier studies that precipitation variance is amplified by land–atmosphere feedback over regions that are least affected by SST (see Koster et al., 2000). Therefore, it is possible that higher decrease in precipitation over the northwest of India, which is far away from the influence of SST is dominated by local land surface processes.

As the monsoon circulation in the PLCS experiment is relatively weaker than in the PLC experiment and SSTs are cooler, large-scale moisture flux into the monsoon domain is also expected to be less. Therefore, changes in rainfall over land would better reflect the impact of local land–atmosphere feedbacks due to LULCC. It is evident from Fig. 6b that there is indeed a significant reduction in seasonal rainfall in PLCS, and over a much wider area of CI and the Western Ghats region than in PLC. Enhancement of rainfall is also evident over some parts of the north and west of India that depict an increase in forests. Maximum decrease in seasonal rainfall (about 3–4 cm) occurs over most parts of CI. Decrease in large-scale moisture convergence in the PLCS experiment is also much widespread extending up to the Arabian Sea, and stronger than in PLC experiment (as evident from denser dashed contours).

### 4.2.1 Changes in frequency of daily rainfall and intensity

We shall study next how changes in seasonal rainfall over CI are also associated with the changes in daily rainfall in the moderate and extreme category. We adopted the criteria for determining thresholds for categorizing moderate and extreme daily rainfall events over CI in the model, that is not exactly the same but is consistent with the method of Goswami et al., 2006. Any daily rainfall total averaged in a grid box is considered as an event. Percentiles of observed (IMD) daily rainfall over CI during JJAS are calculated for the period 1982 till 2007 to identify the value that corresponds to the range of moderate rainfall and lower threshold of extreme rainfall events (see

Sect. 3.3). The observed percentiles are then compared with those calculated for the model to categorize daily moderate and extreme rainfall events in the model. In this way, moderate (extreme) events are identified in the model when $5.34 <$ daily rainfall $\leq 41.72\,\text{mm}\,\text{day}^{-1}$ (daily rainfall $> 59.94\,\text{mm}\,\text{day}^{-1}$). Figure 7a (Fig. 7b) depicts the difference in total number of moderate rainfall events (intensity of rainfall in moderate category) between PLC and HLC experiments during JJAS from 1982 till 2008. Note that for PLC, there is a significant and widespread decrease over CI and the spatial pattern coincides with the increase in crop PFTs in PLC experiment. It may also be noted, that the pattern of decrease matches very well with that of the changes in seasonal rainfall. Following the above methodology, moderate (extreme) rainfall events are identified in the PLCS and HLCS experiments when $4.97 <$ daily rainfall $\leq 41.62\,\text{mm}\,\text{day}^{-1}$ (daily rainfall $> 59.80\,\text{mm}\,\text{day}^{-1}$). The spatial pattern of changes depict that this decrease takes place over a larger part of CI as well as the BI domain (shown in Fig. 4b). On the contrary, changes in extreme rainfall events or the intensity of rainfall in that category are not found to be significant between PLC and HLC or between PLCS and HLCS, whether looked at spatially (figure not shown) or in an aggregated sense over CI.

The mean decrease in the number of moderate rainfall events between PLC and HLC (PLCS and HLCS) is 388 (450), which is significant at the 90 % level of significance. Over the larger BI domain, decrease in moderate rainfall events between PLC and HLC is even greater and is about 642 (significant at 95 %). We note that the order of decrease is comparable to the observed decrease in the number of moderate rainfall events over CI (about 500) in the last 55 years. Along with the number of events, intensity of rainfall amount in a season in the moderate category also decreases significantly at the 95 % level of significance. The decrease in number of moderate events and corresponding rainfall intensity between PLCS and HLCS is even greater, aided by further reduction in large-scale convergence of moisture apart from local land–atmosphere feedbacks. The additional set of sensitivity experiments with de-trended SSTs further help in establishing our hypothesis. As moderate rainfall events constitute a major portion of the seasonal (JJAS) rainfall, we conclude that decrease in seasonal mean rainfall over CI is mainly attributed to differences in the moderate rainfall category due to increase in crop PFTs. Inclusion of light rainfall events ($1 <$ daily rainfall $<$ 5.34 mm day$^{-1}$) in the experiments along with the moderate category does not change our result. We further investigate changes in surface temperature over land and other associated fluxes in order to better understand the above large-scale changes.

## 4.3 Changes in surface air temperature

### 4.3.1 PLC and HLC experiments

Daily 2 m mean air temperature during JJAS in PLC is warmer than HLC by a maximum of 0.3 °C over CI and parts of south (Fig. 8a), which is relatively less than the observed increase. A significant increase in daily maximum temperature (0.4 °C) over the same region as in the mean is also evident (Fig. 8b). The pattern of increase does coincide with increase in crop fraction in PLC (Fig. 1f). Widespread warming is also seen beyond the dry northwestern region of India where the increase in fraction of crop PFTs is more than over CI. Significant cooling is found along a thin belt of the Himalayan foothills in the north that may be attributed to an increase in precipitation (see Fig. 4) as well as changes in albedo and net radiation. A decrease in mean and extreme temperature over small regions of western India is attributed to an increase in forest PFTs (Fig. 1e). At night, the land surface gets de-coupled from the overlying atmosphere on account of cooling, is capped by a layer of inversion and the effect of land surface processes or vegetation on 2 m temperature is minimized. Therefore, and as discussed in Kothawale et al. (2010), the increase in daily mean temperature is mostly dominated by the increase in daily maximum temperature. However, we also noted an increase in temperature at 925 the hPa level (figure not shown), implying that the surface warming extends further up to the depth of the boundary layer.

Apart from changes in the mean temperature, there are also changes in the variability of daily mean and maximum temperature as evident from Fig. 9a and b. There is significant increase in temperature variability over the central and eastern part of India that is attributed to LULCC as well as changes in surface net radiation and advection of moisture and heat. Increase in the variance of extreme is more widespread than in the mean. As the mean and variance of daily surface temperature are altered over CI, it is expected that daily extremes will also change. In order to find out the differences in the extreme temperatures, percentiles are calculated using a time series of 122 days for 27 years (June–September 1982–2008). Difference in the 90th percentiles of daily mean and maximum temperature (in JJAS) between and PLC and HLC is shown in Fig. 9c and d. The 90th percentiles represent the higher temperature extremes attained within the season in the PLC and HLC experiment. The higher extreme values of both daily mean and maximum temperature are about 1 °C more in the PLC experiment over CI. We note that the area of increase coincides very well with the region of maximum increase in the fraction of crop PFTs from 1950 to 2005 (Fig. 1f). It is also interesting to note that the higher extremes get hotter by the same order as depicted in observations. Apart from that, the model does not capture the observed warming over the northwest and peninsular India despite changes in the LULC. Over the northwest of India, the mean as well as extreme temperatures decrease on account of an increase in forest cover over a small region (Fig. 1e).

We further analyzed changes in other surface variables and cloud cover during JJAS to better understand the causes for surface temperature changes due to LULCC. The black contours in Fig. 10 represent the JJAS mean value from the PLC experiment, while the values in shaded show the difference. Areas enclosed within green contours depict significant changes. One would expect the surface pressure over land to decrease and an increase in the land-ocean temperature gradient in the PLC experiment on account of an increase in the surface temperature. However, from Fig. 10a it is evident that surface pressure has increased over most of north, northwest and the Gangetic plains of India. Although a part of CI and its west, the region that captures the monsoon trough (Fig. 6b) and has the lowest surface pressure during JJAS, shows a decrease, the changes are not significant. Therefore, such changes in surface pressure are not responsible for the increase in surface wind speed, but changes in roughness length are. There is also a significant decrease in surface soil moisture (Fig. 10b) associated with the decrease in precipitation, and specific humidity at 2 m (Fig. 10c) over those regions where the fraction of crop PFTs has increased.

We note a significant increase in surface albedo over the land part (Fig. 10d) that is attributed to the increase in crop PFTs and reduction in precipitation that leads to drier soils. However the changes are much less compared to the mean albedo. An increase in albedo would tend to reduce the surface temperature. However, we also note that the percentage of cloud cover has decreased significantly over a large part of CI, the west, north and peninsular India (Fig. 10e). This conforms to the reduction in seasonal precipitation. Due to reduction in cloud cover, there is an increase in surface Net Radiation (NRAD) over those regions, although changes are not significant over CI (Fig. 10f). The increase (decrease) in NRAD over central and southern India (the Himalayan foothills) is contributed by a significant increase (decrease) in net shortwave (SW) radiation (in both net SW and long wave (LW) radiation). Over CI, decrease in net LW radiation partly compensates for the increase in net SW radiation (figure not shown). Decrease in net LW radiation dominates over the northwest of India. We note significant enhancement (reduction) in the mean surface sensible heat flux (SHF) in the PLC experiment over those areas that show an increase in crop (forest) cover (Fig. 10g). On the contrary, the latent heat flux (LHF) that is directly associated with the total evapotranspiration shows a significant change in the opposite sense (Fig. 10h), leading to an overall enhancement in the Bowen Ratio. Therefore, we infer that an increase in NRAD and SHF dominates over changes in surface albedo south of 30° N (towards the Tropics) that also conforms to conclusions in earlier studies (Lawrence and Chase, 2010; Sampaio et al., 2007; Davin and Noblet-Ducoudre, 2010).

It is interesting to note that about 30 % of the decrease in ET (or LHF) over CI, west and southern India (Fig. 10h) is mainly contributed by a reduction in transpiration from vegetation and evaporation of canopy-intercepted water due to LULCC (Fig. 10i). Although this decrease is relatively more over eastern India than towards the center, enhanced ground evaporation arising from increased precipitation partly compensates for that. As a result changes in total ET are not significant towards the east. Therefore, due to a reduction in surface ET, the increased NRAD absorbed at the surface over central and southern India is used up in enhancing the SHF and that further contributes to the increase in mean and higher extreme surface temperatures during JJAS. As mentioned earlier, the daily spatio-temporal variability of surface temperature may be attributed to local thermodynamic effects due to changes in low-level moisture and surface fluxes as well as large-scale dynamics. In this regard, we note that our inferences differ from earlier studies that showed a decrease in growing season surface temperatures over India due to irrigated crops (e.g. Sen Roy et al., 2007; Lee et al., 2009) because we did not use any parameterization scheme for irrigation. Irrigation provides an enhanced source of soil moisture, and hence cools the surface due to evaporation.

### 4.3.2 PLCS and HLCS experiment

We find similar changes when simulated surface temperatures in the remaining two experiments are analyzed. Daily 2 m mean as well as maximum temperature is significantly enhanced in the PLCS experiment by maximum of 0.5 °C, but over a much larger area covering central and southern part of India compared to HLCS (Fig. 11a and b). We note that the increase in temperature over CI is greater and widespread than in earlier experiments. Likewise, over the northwest of India, the spatial pattern of increase extends further to the north and shows greater increase (0.5 °C) in the maximum. Significant cooling is also evident over western and northern India over those areas that show increase in forest cover. The higher extremes (90th percentile) of the daily mean (maximum) temperature have also increased in the PLCS experiment by 1.2 °C (1.0 °C), which is greater than in earlier set of experiments (Fig. 11c and d). Increase in extreme temperature in the PLCS experiment extends further to the west and hence covers a much larger part of CI than in the PLC experiment. We also note that the order of increase in temperature as evident from these two experiments is comparable to that inferred from observations.

There is a significant and widespread decrease in surface soil moisture, specific humidity and LHF and increase in NRAD and sensible heat flux that contributes toward the increase in surface temperature in PLCS experiment (figure not shown). It may be noted that in both set of experiments, the increase in surface temperature is slightly towards south of the area that depicts increase in observation. Apart from that, mean monsoonal features in PLCS experiment convey that there is a decrease in large-scale moisture flow as well as precipitation over the land. As a result alterations in surface fluxes and radiation have a greater impact on changes in air temperature in these additional experiments. Therefore, our experiments with de-trended SST further confirm the proposition that LULCC has partly contributed to the observed increase in surface temperature.

### 4.4 Physical mechanisms

After analyzing changes in local surface variables and the large-scale in the model, one pertinent question arises. How does LULCC lead to reduction in moderate rainfall events? Calculations based on regression show that evapotranspiration over land controls about 10–20 % of the interannual variability in rainfall over CI (Saha et al., 2012). In another study (Halder et al., 2015) we found that surface ET can strongly modulate the terrestrial segment of land–atmosphere coupling strength (Dirmeyer, 2011) for precipitation during the Indian summer monsoon. We note, that in the PLC experiment, decrease in total evapotranspiration over CI is around 3 cm (when LHF in $\mathrm{W\,m^{-2}}$ is converted to $\mathrm{mm\,day^{-1}}$) that constitutes about 40–60 % of the maximum decrease in total rainfall. Although an increase (decrease) in crops (forests) increases the temperature near the surface and within the boundary layer, the associated decrease in local moisture flux could possibly also lower the large-scale convective instability. Vertically integrated moist static energy (VIMSE) is a good measure of instability and precipitation in the Tropics (Srinivasan et al., 1996). VIMSE from surface to 500 hPa during JJAS depicts high values over those areas of land that show maximum seasonal mean rainfall (Fig. 12a). There is a large-scale reduction in VIMSE in the PLC experiment, with significant decrease over a major part of CI and the north (Fig. 12b). Difference in the vertical profile of dry static energy (DSE, blue line) depicts an increase in temperature at the lower levels of atmosphere over CI. Despite that, the effect of decrease in moisture effectively reduces the MSE (red line, Fig. 12c) thereby increasing atmospheric stability and hence lowers the chances of triggering of moist convection over land in the PLC experiment. Lesser large-scale low-level moisture convergence over the land part on account of a reduction in surface roughness length (Fig. 6b) also contributes to the reduced convective instability. These two factors together reduce rainfall in the moderate category.

## 5 Discussions

LULCC in the form of extensive cropland and pasture expansion and deforestation have taken place over India ever since the inception of the Green revolution in the 1960's, associated with urbanization and industrialization. This study explores the hypothesis how LULCC over India has contributed to the observed decrease in moderate rainfall events and increase in extreme surface temperatures during the monsoon season. A RCM, on account of its dynamical downscaling capability and better representation of land–atmosphere feedbacks over the monsoon region has been used to prove the hypothesis. The statistics of the differences between the simulations with fixed present day and historical land cover demonstrate the impact of LULCC on daily surface temperature and precipitation variability during the monsoon (JJAS). Another two similar experiments are also made, but with SSTs de-trended over the ocean in order to eliminate the effect of warming trend in SSTs on temperature and precipitation changes over land. The climatological mean features of Indian summer monsoon are very well captured by the RCM.

Differences show that seasonal rainfall and large-scale moisture convergence is significantly decreased in the PLC and PLCS experiments when compared to the HLC and HLCS experiments, respectively. The decrease is enhanced in case of the PLCS experiment. That decrease in seasonal rainfall is mostly contributed by a significant decrease in moderate rainfall events and amount. Changes in extreme rainfall events are not significant. We demonstrate that a significant increase in surface wind speed over land on account of reduction in surface roughness length is responsible for the decrease in moisture convergence. This is the dynamical response to LULCC. Decrease in forest cover also reduces the regional moisture flux emanating from the surface significantly. Therefore, despite significant increase in surface and low-level temperature, decrease of moisture reduces the large-scale convective instability and chances of precipitation over central and north India. This effect constitutes the thermodynamic response. A decrease in total cloud cover increases the surface Net Radiation that results in an increase in the surface sensible heat flux and the Bowen ratio. Together, they contribute to the increase in surface temperature extremes. It is important to note that the order of increase in surface temperature extremes is comparable to that of observed changes when de-trended SSTs are used. Likewise, the order of decrease in moderate rainfall events also become comparable to observed changes in the period 1951–2005.

It is important to note choice of the model parameterization schemes, accuracy of the lateral boundary conditions and the criteria for calculating thresholds for daily moderate and extreme rainfall events have an influence on the results. Apart from that, the model's grid resolution is about half of that of IMD rainfall data. Hence area of a single grid box in IMD data (which represents an event) is about four times of that of the model. This could also be one of the reasons for disparity in the number of moderate rainfall events between observations and the model. There is a cold temperature bias over land in the model, and positive rainfall bias over the ocean (figure not shown). Apparently, in all these experiments the global warming signal is also present in the large-scale LBCs used from NCEP/NCAR reanalysis that force the model in one way only. A part of the simulated surface temperature and rainfall in the model may also be attributed to non-linear interactions (internal variability) that is model dependent. However, we expect the differences between two simulations with the same model to reduce the effect of these factors and demonstrate the impact of LULCC. Use of a high-resolution RCM is more advantageous in excluding large-scale remote feedbacks that take place in a coarse-resolution GCM and helps better resolve regional land surface processes. Apart from that, we believe that the LULC data prepared from multiple sources and used as fixed lower boundary condition is much improved compared to other historical reconstructed data (such as that of Ramankutty et al., 2008), although there may be certain level of uncertainty in their estimates, particularly during pre-satellite era. However there is no ambiguity about a continuous decrease in forest cover over the last many decades over the south Asian region. Nonetheless, our experiments show that the decrease in moderate rainfall events over India is partly attributed to changes in LULC from 1950 to 2005.

## 6 Conclusions

Apart from an accelerated warming trend in the global mean surface temperature in the later half of the 20th century, the number of extreme events in terms of temperature as well as precipitation has been reported to increase. As regional or local changes in these extremes in different seasons can have different signatures due to complex regional feedbacks associated with the GHGs, clouds, aerosols and other anthropogenic activities, they need greater attention and proper attribution. Regional land–atmosphere feedbacks associated with LULCC are one of the potential drivers of climate change. LULC data shows significant decrease (increase) in the forest (crop) cover over central, south and northwest part of India between 1951 and 2005. From 1951 till 2005, mean (extreme) surface temperature has increased by a maximum of 1.11 °C (1.48 °C). There have also been significant changes in the rainfall distribution during last 55 years over central India. Observed extreme precipitation events have been increasing over central India during the monsoon season and have been potentially associated with the significant warming trend over the Indian Ocean. However, due to significant decrease in moderate rainfall events, the overall seasonal rainfall has reportedly remained stable over India during the 55-year period. In this study, we demonstrate that observed LULC over India has partly contributed to the observed decrease in moderate rainfall events and increase in extreme surface temperature during the monsoon season.

In order to examine whether changes in surface temperature and rainfall distribution pattern are linked with changes in LULC, two sets of long simulations (27 years) using PFTs of 1950 and 2005 as fixed lower boundary condition are carried using the regional climate model RegCM4.0 coupled with the CLM3.5 land surface model. Model simulations with PFT distribution of 1950 and 2005 are referred to as HLC and PLC experiments respectively. Another two sensitivity experiments with similar model set-up are conducted, but with de-trended SSTs over the ocean in order to remove the effect of warming. They are respectively named as PLCS (with 2005 PFTs) and HLCS (with 1950 PFTs) experiments. It is found that, increase in mean and extreme temperatures by 1–1.2 °C over CI in PLC experiment coincides with the region of decrease (increase) in forest (crop) type of PFTs. Furthermore, that increase is found to be even higher and more widespread over the Indian land mass in the PLCS experiment.

Reduction in local evapotranspiration followed by an increase in surface sensible heat flux and Bowen ratio in the PLC experiment is consistent with the decrease in forest cover. Furthermore, wind speed at the lower atmospheric levels increase significantly in the PLC experiment that suggests a decrease in the large-scale moisture convergence over land. Therefore, there is a net decrease in moisture supply over land in PLC as compared to the HLC experiment. Apart from that, decrease in local moisture supply also significantly reduces the large-scale convective instability over land and formation of clouds. Net radiation is increased and that contributes to the increase in surface sensible heat flux and temperature extremes. As the major part of monsoon rainfall occurs through moderate events (about 85 %), it is expected that decrease in total moisture flux and large-scale convective instability over land would also decrease the moderate rainfall events. The model results indeed support that theory, and show that regions with decrease in forest cover depict decrease the number of moderate events as well as the quantity of total rainfall in that category. Changes in heavy rainfall events that are more determined by large-scale moisture availability and triggered by local instabilities, are not significant. These results are further supported by the two additional sensitivity experiments PLCS and HLCS. Availability of local surface moisture flux that is associated with the type of LULC is crucial in determining the changes in large-scale instability over land and hence chances of convective triggering of rainfall. Therefore, this study demonstrates that LULC changes in the last 55 years have contributed partly to the observed decrease in moderate rainfall events over India as well as increase in extreme surface temperatures.

Understanding the mechanisms responsible for observed changes in extreme surface temperature and rainfall distribution in the monsoon regions is important for the scientific community and policy makers as well. It is conceivable that, as the global mean temperature becomes warmer and the climate unpredictable, LULC change due to population growth, deforestation/afforestation, agricultural expansion and urbanization would add more uncertainties through its dynamic (e.g. strength of large-scale circulation) and thermodynamic effects (albedo, evaporation and instability changes). Effect of urbanization is expected to increase warming, reduce local evaporation and also possibly affect rainfall distribution. However, this study does not include urbanization effects. Apart from that, impact of aerosols and irrigation activity has also not been considered which would introduce competing influences. Therefore part of the regional warming seen in observations could not be explained only through changes in LULC that we have isolated here. It would be interesting to study in future the effect of LULC change in a high-resolution global model where the effect of other anthropogenic forcing are included, and also where the LULC changes with time or dynamic vegetation is used. Nevertheless, this study shows that it is highly important to include projected anthropogenic changes in regional LULC in IPCC future climate change scenarios.

**The Supplement related to this article is available online at doi:10.5194/hessd-12-6575-2015-supplement.**

*Acknowledgements.* Authors thank the Abdus Salam International Centre for Theoretical Physics in Trieste, Italy for making the model codes of RegCM4.0 available for this study from http://gforge.ictp.it/gf/. Global time varying forcing datasets for the RCM and fixed datasets for the CLM3.5 land surface model are obtained from http://users.ictp.it/pubregcm/RegCM3/globedat.htm. The PFT based global vegetation datasets were prepared at the Cooperative Institute for Research in Environmental Sciences, University of Colorado at Boulder, USA. Daily high-resolution gridded rainfall (Product No. 1/2005) and temperature data (Product No. 3/2008) which are prepared from quality controlled station observations can be purchased for a fee from the National Climate Centre (NCC), IMD, Pune, India. Details about the procedure of purchase can be searched in the link “NCC Gridded Data Product”, present in the webpage http://www.imdpune.gov.in/publication/pub_index.html. The figures have been prepared using the freely available software package GrADS.

Authors gratefully acknowledge the use of data and resources at the Indian Institute of Tropical Meteorology (IITM), Pune, India. Fellowship of S. Halder was funded by the CSIR, New Delhi, India during completion of this study for his PhD thesis while at IITM. S. Halder and P. Dirmeyer are supported by a grant from the Ministry of Earth Sciences (India) to the Center for Ocean-Land–Atmosphere Studies of George Mason University. Support for the Twentieth Century Reanalysis Project dataset is provided by the U.S. Department of Energy, Office of Science Innovative and Novel Computational Impact on Theory and Experiment (DOE INCITE) program, and Office of Biological and Environmental Research (BER), and by the National Oceanic and Atmospheric Administration Climate Program Office.

## References

Adler, R. F., Huffman, G. J., Chang, A., Ferraro, R., Xie, P., Janowiak, J., Rudolf, B., Schneider, U., Curtis, S., Bolvin, D., Gruber, A., Susskind, J., and Arkin, P.: The version 2 Global Precipitation Climatology Project (GPCP) monthly precipitation analysis (1979–present), J. Hydrometeorol., 4, 1147–1167, doi:10.1175/1525-7541(2003)004<1147:TVGPCP>2.0.CO;2, 2003.

Alexander, L. V., Zhang, X., Peterson, T. C., Caesar, J., Gleason, B., Tank, A. M. G. K., Haylock, M., Collins, D., Trewin, B., Rahimzadeh, F., Tagipour, A., Kumar, K. R., Revadekar, J., Griffiths, G., Vincent, L., Stephenson, D. B., Burn, J., Aguilar, E., Brunet, M., Taylor, M., New, M., Zhai, P., Rusticucci, M., and Vazquez-Aguirre, J. L.: Global observed changes in daily climate extremes of temperature and precipitation, J. Geophys. Res., 111, D05109, doi:10.1029/2005JD006290, 2006.

Ali, H., Misra, V., and Pai, D. S.: Observed and projected urban extreme rainfall events in India, J. Geophys. Res., 19, 12621–12642, doi:10.1002/2014JD022264, 2014.

Allen, M. R. and Ingram, W. J.: Constraints on future changes in climate and the hydrologic cycle, Nature, 419, 224–231, doi:10.1038/nature01092, 2002.

Avila, F. B., Pitman, A. J., Donat, M. G., Alexander, L. V., and Abramowitz, G.: Climate model simulated changes in temperature extremes due to land cover change, J. Geophys. Res., 117, D04108, doi:10.1029/2011JD016382, 2012.

Behera, S. K., Krishnan, R., and Yamagata T: Unusual ocean atmosphere conditions in the tropical Indian ocean during 1994, Geophys. Res. Lett., 26, 3001–3004, doi:10.1029/1999GL010434, 1999.

Bonan, G. B., Oleson, K. W., Vertenstein, M., Levis, S., Zeng, X., Dai, Y., Dickinson, R. E., and Yang, Z.-L.: The land surface climatology of the community land model coupled to the NCAR community climate model, J. Climate, 15, 3123–3149, doi:10.1175/1520-0442(2002)015<3123:TLSCOT>2.0.CO;2, 2002.

Bounoua, L., DeFries, R., Collatz, G. J., Sellers, P., and Khan, H.: Effects of land cover conversion on surface climate, Climatic Change, 52, 29–64, 2002.

Chow, K. C., Cha, J. C. L., Pal, J. S., and Giorgi, F.: Convection suppression criteria applied to the MIT cumulus parameterization scheme for simulating the Asian summer monsoon, Geophys. Res. Lett., 32, L24709, doi:10.1029/2006GL028026, 2006.

Chowdary, J. S., John, N., and Gnanaseelan, C.: Interannual variability of surface air-temperature over India: impact of ENSO and Indian Ocean Sea surface temperature, Int. J. Climatol., 34, 2, 416–429, doi:10.1002/joc.3695, 2013.

Compo, G. P., Whitaker, J. S., Sardeshmukh, P. D., Matsui, N., Allan, R. J., Yin, X., Gleason, B. E., Vose, R. S., Rutledge, G., Bessemoulin, P., Bronnimann, S., Brunet, M., Crouthamel, R. I., Grant, A. N., Groisman, P. Y., Jones, P. D., Kruk, M. C., Kruger, A. C., Marshall, G. J., Maugeri, M., Mok, H. Y., Nordli Ø., Ross, T. F., Trigo, R. M., Wang, X. L., Woodruff, S. D., and Worleyu, S. J.: Review article: the Twentieth Century Reanalysis Project, Q. J. Roy. Meteor. Soc., 137, 1–28, doi:10.1002/qj.776, 2011.

Davin, E. L. and De Noblet-Ducoudrè, N.: Climatic impact of global-scale deforestation: radiative versus nonradiative processes, J. Climate, 23, 97–112, 2010.

Dirmeyer, P. A.: The terrestrial segment of soil moisture-climate coupling, Geophys. Res. Lett., 38, 16, doi:10.1029/2011GL048268, 2011.

Dirmeyer, P. A., Niyogi, D., de Noblet-Ducoudrè, N., Dickinson, R. E., and Snyder, P. K.: Editorial: impacts of land use change on climate, Int. J. Climatol., 30, 1905–1907, 2010.

Douglas, E. M., Niyogi, D., Frolking, S., Yeluripati, J. B., Pielke Sr., R. A., Vorosmarty, C. J., and Mohanty, U. C.: Change in moisture and energy fluxes due to agricultural land use and irrigation in the Indian monsoon belt, Geophys. Res. Lett., 33, L14403, doi:10.1029/2006GL026550, 2006.

Dutta, S. K., Das, S., Kar, S. C., Mohanty, U. C., and Joshi, P. C.: Impact of vegetation on the simulation of seasonal monsoon rainfall over the Indian subcontinent using a regional model, J. Earth Syst. Sci., 118, 5, 413–440, 2009.

Elguindi, N., Bi, X., Giorgi, F., Nagarajan, B., Pal, J., Solmon, F., Rauscher, S., and Zakey, A.: RegCM version 4.0 User's Guide, ICTP, Trieste, Italy, available at: gforge.ictp.it/gf/download/docmanfileversion/6/253/UserGuide.pdf, last access: June 2015, 2010.

Feddema, J., Oleson, K., Bonan, G., Mearns, L., Washington, W., Meehl, G., and Nychka, D.: A comparison of a GCM response to historical anthropogenic land cover change and model sensitivity to uncertainty in present-day land cover representations, Clim. Dynam., 25, 581–609, doi:10.1007/s00382-005-0038-z, 2005.

Feser, F. and Barcikowska, M.: The influence of spectral nudging on typhoon formation in regional climate models, Environ. Res. Lett., 7, 014024, doi:10.1088/1748-9326/7/1/014024, 2012.

Feser, F., Rockel, B., von Storch, H., Winterfeldt, J., and Zahn, M.: Regional climate models add value to global model data: a review and selected examples, B. Am. Meteorol. Soc., 92, 1181–1192, doi:10.1175/2011BAMS3061.1, 2011.

Frei, C., Christensen, J. H., De'que', M., Jacob, D., Jones, R. G., and Vidale, P. L.: Daily precipitation statistics in regional climate models: evaluation and intercomparison for the European Alps, J. Geophys. Res., 108, 4124, doi:10.1029/2002JD002287, 2003.

Fritsch, J. M. and Chappell, C. F.: Numerical prediction of convectively driven mesoscale pressure systems. Part I: Convective parameterization, J. Atmos. Sci., 37, 1722–1733, doi:10.1175/1520-0469(1980)037<1722:NPOCDM>2.0.CO;2, 1980.

Garratt, J. R.: Sensitivity of climate simulations to land-surface and atmospheric boundary layer treatments – a review, J. Climate, 6, 419–449, doi:10.1175/1520-0442(1993)006<0419:SOCSTL>2.0.CO;2, 1993.

Gao, X., Shi, Y., Zhang, D., Wu, J., Giorgi, F., Ji, Z., and Wang, Y.: Uncertainties in monsoon precipitation projections over China: results from two high-resolution RCM simulations, Clim. Res., 52, 213–226, 2012.

Giorgi, F. and Bates, G. T.: The climatological skill of a regional model over complex terrain, Mon. Weather Rev., 117, 2325–2347, 1989.

Giorgi, F., Coppola, E., Solmon, F., Mariotti, L., Sylla, M. B., Bi, X., Elguindi, N., Diro, G. T., Nair, V., Giuliani, G., Turuncoglu, U. U., Cozzini, S., Guttler, I., O'Brien, T. A., Tawfik, A. B., Shalaby, A., Zakey, A. S., Steiner, A. L., Stordal, F., Sloan, L. C., and Brankovic, C.: RegCM4: model description and preliminary tests over multiple CORDEX domains, Clim. Res., 52, 7–29, doi:10.3354/cr01018, 2012.

Goldewijk, K. K.: Estimating global land use change over the past 300 years: the HYDE database, Global Biogeochem. Cy., 15, 417–433, 2001.

Goswami, B. N., Venugopal, V., Sengupta, D., Madhusoodanan, M. S., and Xavier, P. K.: Increasing trend of extreme rain events over India in a warming environment, Science, 314, 1442–1445, doi:10.1126/science.1132027, 2006.

Grell, G. A.: Prognostic evaluation of assumptions used by cumulus parameterization, Mon. Weather. Rev., 121, 764–787, doi:10.1175/1520-0493(1993)121<0764:PEOAUB>2.0.CO;2, 1997.

Halder, S., Dirmeyer, P., and Saha, S. K.: Uncertainty in the mean and variability of Indian summer monsoon due to land atmosphere feedback in RegCM4, J. Geophys. Res., in review, 2015.

Haerter, J. O. and Berg, P.: Unexpected rise in extreme precipitation caused by a shift in rain type?, Nat. Geosci., 2, 372–373, doi:10.1038/ngeo523, 2001.

Holtslag, A. A. M., Bruijn, E. I. F. D., and Pan, H. L.: A high resolution air mass transformation model for short-range weather forecasting, Mon. Weather. Rev., 118, 1561–1575, doi:10.1175/1520-0493(1990)118<1561:AHRAMT>2.0.CO;2, 1999.

Hurtt, G. C., Frolking, S., Fearon, M., Moore, B., Shevliakova, E., Malyshev, S., Pacala, S., and Houghton, R.: The underpinnings of land-use history: three centuries of global gridded land-use transitions, wood-harvest activity, and resulting secondary lands, Glob. Change Biol., 12, 1208–1229, doi:10.1111/j.1365-2486.2006.01150.x, 2006.

Jaswal, A., Rao, G. P., and De, U.: Spatial and temporal characteristics of evaporation trends over India during 1971–2000, Mausam, 59, 149–158, 2008.

Jaswal, A. K., Rao, P. C. S., and Singh, V.: Climatology and trends of summer high temperature days in India during 1969–2013, J. Earth Syst. Sci., 124, 1–15, 2015.

Kalnay, E., Kanamitsu, M., Kistler, R., Collins, W., Deaven, D., Gandin, L., Iredell, M., Saha, S., White, G., Woollen, J., Zhu, Y., Leetmaa, A., Reynolds, R., Chelliah, M., Ebisuzaki, W., Higgins, W., Janowiak, J., Mo, K. C., Ropelewski, C., Wang, J., Jenne, R., and Joseph, D.: The NCEP/NCAR 40-year reanalysis project, B. Am. Meteorol. Soc., 77, 437–470, 1996.

Kang, I.-S., Yang, Y. M., and Tao, W. K.,: GCMs with implicit and explicit representation of cloud microphysics for simulation of extreme precipitation frequency, Clim. Dynam., 45, 325–335, doi:10.1007/s00382-014-2376-1, 2014.

Karl, T. R., Jones, P. D., Knight, R. W., Kukla, G., Mummer, N., Razuvayev, V., Gallo, K. P., Lindseay, J., Charlson, R. J., and Peterson, T. C.: Asymmetric trends of daily maximum and minimum temperature, B. Am. Meteorol. Soc., 74, 6, 1007–1023, 1993.

Kiehl, J. T., Hack, J. J., Bonan, G. B., Boville, B. A., Briegleb, B. P., Williamson, D. L., and Rasch, P. J.: Description of the NCAR Community Climate Model (CCM3), NCAR, Boulder, Colorado, USA, Tech. Rep., NCAR, NCAR/TN-420+STR, 1996.

Kishtawal, C., Niyogi, D., Tewari, M., Pielke Sr., R. A., and Shepherd, M.: Urbanization signature in the observed heavy rainfall climatology over India, Int. J. Climatol., 30, 1908–1916, doi:10.1002/joc.2044, 2010.

Koster, R. D., Suarez, M. J., and Heiser, M.: Variance and predictability of precipitation at seasonal-to-interannual timescales, J. Hydrometeorol., 1, 26–46, doi:10.1175/1525-7541(2000)001<0026:VAPOPA>2.0.CO;2, 2001.

Kothawale, D. R. and Rupa Kumar, K.: On the recent changes in surface temperature trends over India, Geophys. Res. Lett., 32, L18714, doi:10.1029/2005GL023528, 2005.

Kothawale, D. R., Munot, A. A., and Kumar, K. K.: Surface air temperature variability over India during 1901–2007, and its association with ENSO, Clim. Res., 42, 89–104, doi:10.3354/cr00857, 2010.

Laprise, R., de Elía, R., Caya, D., Biner, S., Lucas-Picher, P., Diaconescu, E., Leduc, M., Alexandru, A., and Separovic, L.: Challenging some tenets of regional climate modeling, Meteorol. Atmos. Phys., 100, 3–22, 2008.

Lawrence, P. J. and Chase, T. N.: Investigating the climate impacts of global land cover change in the community climate system model, Int. J. Climatol., 30, 2066–2087, doi:10.1002/joc.2061, 2010.

Leduc, M. and Laprise, R.: Regional climate model sensitivity to domain size, Clim. Dynam., 32, 833–854, 2009.

Lee, E., Chase, T. N., Rajagopalan, B., Barry, R. G., Biggs, T. W., and Lawrence, P. J.: Effects of irrigation and vegetation activity on early Indian summer monsoon variability, Int. J. Climatol., 29, 573–581, doi:10.1002/joc.1721, 2009.

Lohar, D. and Pal, B.: The effect of irrigation on premonsoon season over South West Bengal, India, J. Climate, 8, 2567–2570, doi:10.1175/1520-0442(1995)008<2567:TEOIOP>2.0.CO;2, 1995.

Mahmood, R., Pielke Sr., R. A., Hubbard, K., Niyogi, D., Dirmeyer, P., McAlpine, C., Carleton, A., Hale, R., Gameda, S., Beltran-Przekurat, A., Baker, B., McNider, R., Legates, D. R., Shepherd, M., Du, J., Blanken, P., Frauenfeld, O. W., Nair, U. S., and Fall, S.: Land cover changes and their biogeophysical effects on climate, Int. J. Climatol., 34, 929–953, 2010.

Nayak, S. and Mandal, M.: Impact of land-use and land-cover changes on temperature trends over Western India, Curr. Sci. India, 102, 1166–1173, 2012.

Niranjan, Kumar, K., Rajeevan, M., Pai, D. S., Srivastava, A. K., and Preethi, B.: On the observed variability of monsoon droughts over India, Weather and Climate Extremes, 1, 42–50, doi:10.1016/j.wace.2013.07.006, 2013.

Niyogi, D., Kishtawal, C. M., Tripathi, S., and Govindaraju, R. S.: Observational evidence that agricultural intensification and land use change may be reducing the Indian summer monsoon rainfall, Water Resour. Res., 46, W03533, doi:10.1029/2008WR007082, 2010.

Oleson, K. W., Niu, G. Y., Yang, Z. L., Lawrence, D. M., Thornton, P. E., Lawrence, P. J., Stockli, R., Dickinson, R. E., Bonan, G. B., Levis, S., Dai, A., and Qian, T.: Improvements to the Community Land Model and their impact on the hydrological cycle, J. Geophys. Res., 113, G01021, doi:10.1029/2007JG000563, 2008.

Oleson, K. W., Lawrence, D. M., Bonan, G. B., Flanner, M. G., Kluzek, E., Lawrence, P. J., Levis, S., Swenson, S. C., Thornton, P. E., Dai, A., Decker, M., Dickinson, R., Feddema, J., Heald, C. L., Hoffman, F., Lamarque, J. F., Mahowald, N., Niu, G. Y., Qian, T., Randerson, J., Running, S., Sakaguchi, K., Slater, A., Stockli, R., Wang, A., Yang, Z. L., Zeng, X., and Zeng, X.: Technical description of version 4.0 of the Community Land Model (CLM), NCAR, Boulder, Colorado, USA, NCAR Technical Note NCAR/TN-387+STR, NCAR, 257 pp., 2010.

Pai, D. S. and Sridhar, L.: Long term trends in the extreme rainfall events over India, in: High-Impact Weather Events over the SAARC Region, edited by: Ray, K., Mohapatra, M., Bandyopadhyay, B. K., and Rathore, L. S., Springer International Publishing, Cham, Switzerland with Capital Publishing Company, New Delhi, India, 229–240, 2015.

Pai, D. S., Nair, S. A., and Ramanathan, A. N.: Long term climatology and trends of heat waves over India during the recent 50 years (1961–2010), Mausam, 64, 585–604, 2013.

Pal, J. S., Giorgi, F., Bi, X., Elguindi, N., Solmon, F., Gao, X., Rauscher, S. A., Francisco, R., Zakey, A., Winter, J., Ashfaq, M., Syed, F. S., Bell, J. L., Diffenbaugh, N. S., Karmacharya, J., Konar, A., Martinez, D., da Rocha, R. P., Sloan, L. C., and Steiner, A. L.: Regional climate modeling for the developing world: the ICTP RegCM3 and RegCNET, B. Am. Meteorol. Soc., 88, 9, 1395–1409, doi:10.1175/BAMS-88-9-1395, 2007.

Panda, D. K. and Kumar, A.: The changing characteristics of monsoon rainfall in India during 1971–2005 and links with large scale circulation, Int. J. Climate, 3881–3899, doi:10.1002/joc.3948, 2014.

Pielke Sr., R. A.: Influence of the spatial distribution of vegetation and soils on the prediction of cumulus convective rainfall, Rev. Geophys., 39, 151–177, doi:10.1029/1999RG000072, 2001.

Pielke Sr., R. A., Pitman, A., Niyogi, D., Mahmood, R., McAlpine, C., Hossain, F., Goldewijk, K. K., Nair, U., Betts, R., Fall, S., Reichstein, M., Kabat, P., and de Noblet, N.: Land use/land cover changes and climate: modeling analysis and observational evidence, WIREs Climate Change, 2, 828–850, doi:10.1002/wcc.144, 2011.

Pitman, A. J., de Noblet-Ducoudré, N., Avila, F. B., Alexander, L. V., Boisier, J.-P., Brovkin, V., Delire, C., Cruz, F., Donat, M. G., Gayler, V., van den Hurk, B., Reick, C., and Voldoire, A.: Effects of land cover change on temperature and rainfall extremes in multi-model ensemble simulations, Earth Syst. Dynam., 3, 213–231, doi:10.5194/esd-3-213-2012, 2012.

Rajeevan, M., Bhate, J., Kale, J. D., and Lal, B.: High resolution daily gridded rainfall data for Indian region: analysis of break and active monsoon spells, Curr. Sci. India, 9, 296–306, 2006.

Rajeevan, M., Bhate, J., and Jaswal, A. K.: Analysis of variability and trends of extreme rainfall events over India using 104 years of gridded daily rainfall data, Geophys. Res. Lett., 35, L18707, doi:10.1029/2008GL035143, 2008.

Ramankutty, N. and Foley, J. A.: Estimating historical changes in global land cover: croplands from 1700 to 1992, Global Biogeochem. Cy., 13, 997–1027, doi:10.1029/1999GB900046, 1999.

Ramankutty, N., Evan, A. T., Monfreda, C., and Foley, J. A.: Farming the planet: 1. Geographic distribution of global agricultural lands in the year 2000, Global Biogeochem. Cy., 22, GB1003, doi:10.1029/2007GB002952, 2008.

Ratnam, J. V., Giorgi, F., Kaginalkar, A., and Cozzini, S.: Simulation of the Indian monsoon using the RegCM3-ROMS regional coupled model, Clim. Dynam., 33, 119–139, doi:10.1007/s00382-008-0433-3, 2009.

Reynolds, R. W., Rayner, N. A., Smith, T. M., Stokes, D. C., and Wang, W.: An improved in situ and satellite SST analysis for climate, J. Climate, 15, 1609–1625, doi:10.1175/1520-0442(2002)015<1609:AIISAS>2.0.CO;2, 2002.

Roxy, K. M., Kapoor, R., Terray, P., and Masson, S.: The curious case of Indian Ocean warming, J. Climate, 27, 8501–8509, doi:10.1175/JCLI-D-14-00471.1, 2014.

Saeed, F., Hagemann, S., and Jacob, D.: Impact of irrigation on the South Asian summer monsoon, Geophys. Res. Lett., 36, L20711, doi:10.1029/2009GL040625, 2009.

Saha, S. K., Halder, S., Kumar, K. K., and Goswami, B. N.: Pre-onset land surface processes and “internal” interannual variabilities of the Indian summer monsoon, Clim. Dynam., 36, 2077–2089, doi:10.1029/2011JD017291, 2011.

Saha, S. K., Halder, S., Rao, A. S., and Goswami, B. N.: Modulation of ISOs by land–atmosphere feedback and contribution to the interannual variability of Indian summer monsoon, J. Geophys. Res., 117, D1301, doi:10.1029/2011JD017291, 2012.

Sampaio, G., Nobre, C. A., Costa, M. H., Satyamurty, P., Soares-Filho, B. S., and Cardoso, M.: Regional climate change over eastern Amazonia caused by pasture and soybean cropland expansion, Geophy. Res. Let., 34, L17709, doi:10.1029/2007GL030612, 2007.

Sen Roy, S., Mahmood, R., Niyogi, D., Lei, M., Foster, S. A., Hubbard, K. G., Douglas, E., and Pielke Sr., R. A.: Impacts of the agricultural Green Revolution induced land use changes on air temperatures in India, J. Geophys. Res., 112, D21108, doi:10.1029/2007JD008834, 2007.

Sen Roy, S., Mahmood, R., Quintanar, A. I., and Gonzalez, A.: Impacts of irrigation on dry season precipitation in India, Theor. Appl. Climatol., 104, 193–207, doi:10.1007/s00704-010-0338-z, 2011.

Shkol'nik, I., Meleshko, V., Efimov, S., and Stafeeva, E.: Changes in climate extremes on the territory of Siberia by the middle of the 21st century: an ansemble forecast based on the MGO Regional Climate Model, Russ. Meteorol. Hydrol., 37, 71–84, 2012.

Seneviratne, S., Nicholls, N., Easterling, D., Goodess, C. M., Kanae, S., Kossin, J., Luo, Y., Marengo, J., McInnes, K., Rahimi, M., Reichstein, M., Sorteberg, A., Vera, C., and Zhang, X.: Changes in climate extremes and their impacts on the natural physical environment, in: SREX: Special Report on Managing the Risks of Extreme Events and Disasters to Advance Climate Change Adaptation, edited by: Field, C. B., Barros, V., Stocker, T. F., Qin, D., Dokken, D. J., Ebi, K. L., Mastrandrea, M. D., Mach, K. J., Plattner, G.-K., Allen, S. K., Tignor, M., and Midgley, P. M., A Special Report of Working Groups I and II of the Intergovernmental Panel on Climate Change (IPCC), Cambridge University Press, Cambridge, UK and New York, NY, USA, 109–230, 2012.

Sheikh, M. M., Manzoor, N., Ashraf, J., Adnan, M., Collins, D., Hameed, S., Manton, M. J., Ahmed, A. U., Baidya, S. K., Borgaonkar, H. P., Islam, N., Jayasinghearachchi, D., Kothawale, D. R., Premalal, K. H. M. S., Revadekar, J. V., and Shrestha, M.L: Trends in extreme daily rainfall and temperature indices over South Asia, Int. J. Climate, 35, 1625–1637, doi:10.1002/joc.4081, 2014.

Singh, D., Tsiang, M., Rajaratnam, B., and Diffenbaugh, N. S.: Observed changes in extreme wet and dry spells during the South Asian summer monsoon season, Nature Climate Change, 4, 456–461, doi:10.1038/nclimate2208, 2014.

Snyder, P. K.: The influence of tropical deforestation on the Northern Hemisphere climate by atmospheric teleconnections, Earth Interact., 14, 1–32, doi:10.1175/2010EI280.1, 2010.

Solomon, S., Qin, D., Manning, M., Chen, Z., Marquis, M., Averyt, K. B., Tignor, M., and Miller, H. L. (Eds.): Climate Change 2007: The Physical Science Basis. Contribution of Working Group I to the Fourth Assessment Report of the Intergovernmental Panel on Climate Change, Cambridge University Press, New York, 996 pp., 2007.

Srinivasan, J. and Smith, G. L.: The role of heat fluxes and moist static energy in tropical convergence zones, Mon. Weather Rev., 124, 2089–2099, doi:10.1175/1520-0493(1996)124<2089:TROHFA>2.0.CO;2, 1996.

Srivastava, A. K., Rajeevan, M., and Kshirsagar, S. R.: Development of a high resolution daily gridded temperature data set (1969–2005) for the Indian region, Atmos. Sci. Let., 10, 249–254, doi:10.1002/asl.232, 2009.

Stocker, T. F., Qin, D., Plattner, G.-K., Tignor, M., Allen, S. K., Boschung, J., Nauels, A., Xia, Y., Bex, V., and Midgley, P. M. (Eds.): IPCC, 2013: Climate Change 2013: The Physical Science Basis. Contribution of Working Group I to the Fifth Assessment Report of the Intergovernmental Panel on Climate Change, Cambridge University Press, Cambridge, UK and New York, NY, USA, 1535 pp., 2013.

Stockli, R., Lawrence, D. M., Niu, G. Y., Oleson, K. W., Thornton, P. E., Yang, Z. L., Bonan, G. B., Denning, A. S., and Running, S. W.: Use of FLUXNET in the Community Land Model development, J. Geophys. Res., 113, G01025, doi:10.1029/2007JG000562, 2008.

Sud, Y., Shukla, J., and Mintz, Y.: Influence of land surface roughness on atmospheric circulation and precipitation: a sensitivity study with a general circulation model, J. Appl. Meteorol., 27, 1036–1054, doi:10.1175/1520-0450(1988)027<1036:IOLSRO>2.0.CO;2, 1998.

Takata, K., Saito, K., and Yasunari, T.: Changes in the Asian monsoon climate during 1700–1850 induced by preindustrial cultivation, P. Natl. Acad. Sci. USA, 106, 9586–9589, doi:10.1073/pnas.0807346106, 2009.

Tawfik, A. and Steiner, A. L.: The role of soil ice in land–atmosphere coupling over the United States: a soil moisture–precipitation winter feedback mechanism, J. Geophys. Res., 116, D02113, doi:10.1029/2010JD014333, 2011.

Tian, H., Banger, K., Bo, T., and Dadhwal, V. K.: History of land use in India during 1880–2010: large-scale land transfprmations reconstructed from satellite data and historical archives, Global Planet. Change, 121, 76–88, doi:10.1016/j.gloplacha.2014.07.005, 2014.

Trenberth, K. E.: Atmospheric moisture residence times and cycling: implications for rainfall rates and climate change, Climatic Change, 39, 667–694, 1998.

Trenberth, K. E.: Changes in precipitation with climate change, Clim. Res., 47, 123–138, doi:10.3354/cr00953, 2011.

Trenberth, K. E., Dai, A., Rasmussen, R. M., and Parsons, D. B.: The changing character of precipitation, B. Am. Meteorol. Soc., 84, 1205–1217, doi:10.1175/BAMS-84-9-1205, 2003.

Tuinenburg, O. A., Hutjes, R. W. A., Jacobs, C. M. J., and Kabat, P.: Diagnosis of local land–atmosphere feedbacks in India, J. Climate, 24, 251–266, doi:10.1175/2010JCLI3779.1, 2011.

Wang, B., Ding, Q., and Joseph, P. V.: Objective definition of the Indian Summer Monsoon onset, J. Climate, 22, 3303–3316, doi:10.1175/2008JCLI2675.1, 2009.

Willett, K. M., Jones, P. D., Thorne, P. W., and Gillett, N. P.: A comparison of large scale changes in surface humidity over land in observations and CMIP3 general circulation models, Environ. Res. Lett., 5, 025210, doi:10.1088/1748-9326/5/2/025210, 2010.

Xavier, P. K., Marzin, C., and Goswami, B. N.: An objective definition of the Indian summer monsoon season and a new perspective on the ENSO-monsoon relationship, Q. J. Roy. Meteor. Soc., 133, 749–764, doi:10.1002/qj.45, 2007.

Xue, Y., Janjic, Z., Dudhia, J., Vasic, R., and De Sales, F.: A review on regional dynamical downscaling on intraseasonal to seasonal simulation/prediction and major factors that affect downscaling ability, Atmos. Res., 147–148, 68–85, 2014.

Yatagai, A., Kamiguchi, K., Arakawa, O., Hamada, A., Yasutomi, N., and Kitoh, A.: APHRODITE: constructing a long-term daily gridded precipitation dataset for asia based on a dense network of rain gauges, B. Am. Meteorol. Soc., 93, 1401–1415, doi:10.1175/BAMS-D-11-00122.1, 2012.

Zeng, X. and Beljaars, A.: A prognostic scheme of sea surface skin temperature for modeling and data assimilation, Geophys. Res. Lett., 32, L14605, doi:10.1029/2005GL023030, 2005.

Zeng, X., Shaikh, M., Dai, Y., Dickinson, R. E., and Myneni, R.: Coupling of the Common Land Model to the NCAR Community Climate Model, J. Climate, 15, 1832–1854, 2002.

Title Page
Abstract | Introduction
Conclusions | References
Tables | Figures
◀| |▶
◀ ▶
Back | Close
Full Screen / Esc
Printer-friendly Version
Interactive Discussion

**Table 1.** Experimental set-up for LULCC based simulations with RegCM4.

| Experiment name | Lateral boundary conditions | Sea surface temperature | Year of fixed LULC | Period of simulation |
|---|---|---|---|---|
| PLC | 01 Nov 1981–31 Dec 2008 | Observed (1981–2008) | 2005 | 27 years |
| HLC | 01 Nov 1981–31 Dec 2008 | Observed (1981–2008) | 1950 | 27 years |
| PLCS | 01 Nov 1981–31 Dec 2008 | De-trended (1981–2008) | 2005 | 27 years |
| HLCS | 01 Nov 1981–31 Dec 2008 | De-trended (1981–2008) | 1950 | 27 years |

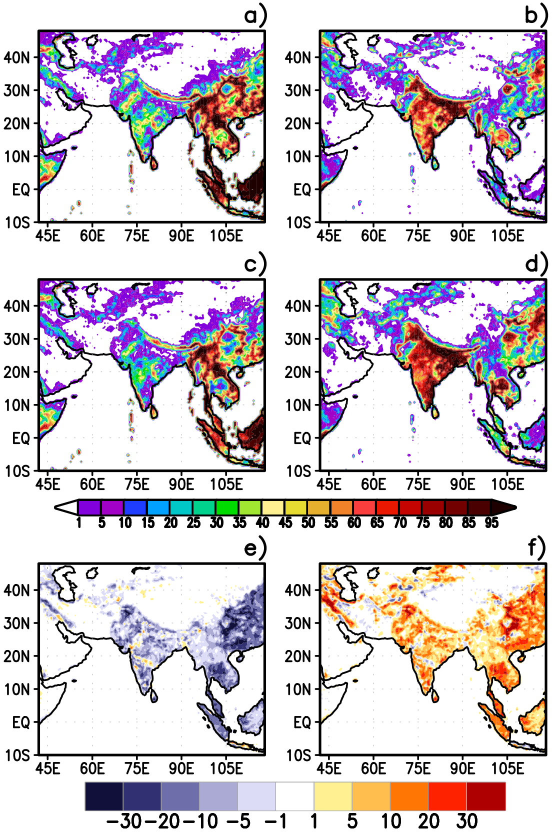

**Figure 1.** PFT distribution of crop and forest cover (in %) used as fixed lower boundary condition in the model experiments. **(a)** Forest and **(b)** crop of the year 1950 (HLC). **(c)** Forest and **(d)** crop of the year 2005 (PLC). Differences (PLC-HLC) in **(e)** forest and **(f)** crop cover.

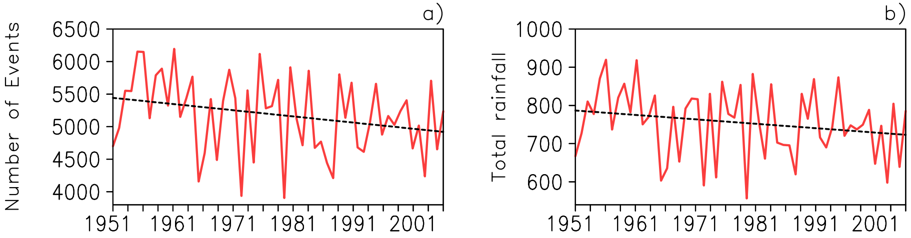

**Figure 2.** Time series of number of observed moderate rainfall events over CI and total rainfall in JJAS (in mm; 1951–2007) from moderate events in IMD rainfall data. **(a)** Moderate rainfall events and **(b)** total amount of rainfall in moderate category. Black dotted line represents the linear trend.

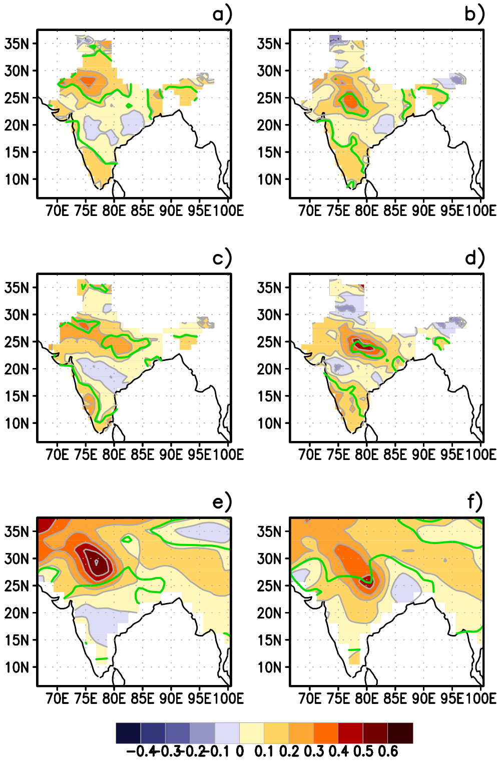

**Figure 3.** Observed trend (1969–2005) in seasonal (JAS) 2 m air temperature from IMD (in °C decade$^{-1}$). Trend in **(a)** seasonal average of daily mean, **(b)** 90th percentile of daily mean, **(c)** seasonal average of daily maximum, and **(d)** 90th percentile of daily maximum temperature. Observed trend (1951–2005) in **(e)** seasonal average of daily mean and **(f)** 90th percentile of daily mean 2 m air temperature from 20CR reanalysis data (in °C decade$^{-1}$). Green contour encloses the region where trends are significant at 90 % confidence level.

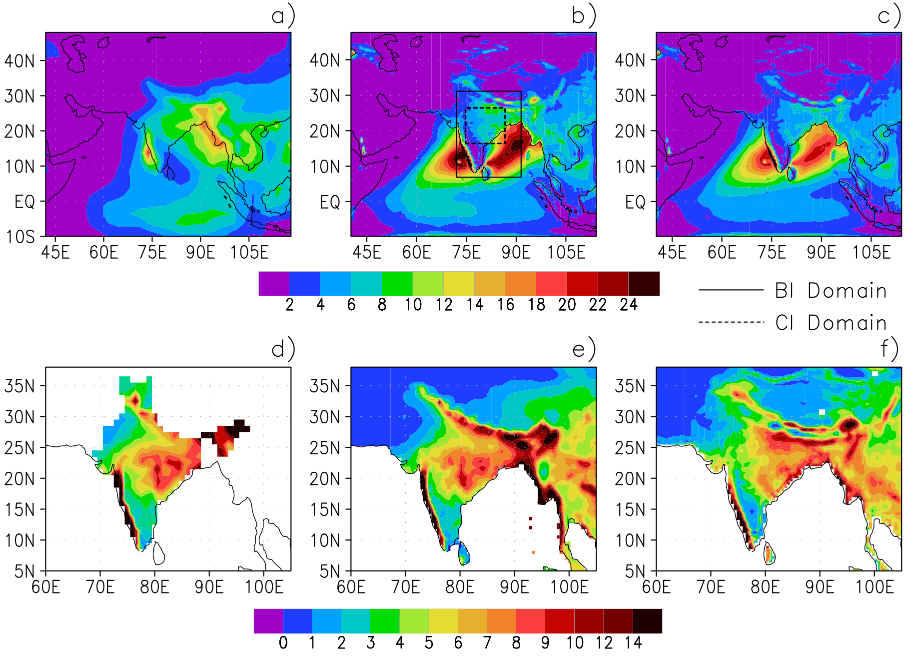

**Figure 4. (a)** Seasonal (JJAS) averaged rainfall from GPCP (in mm day$^{-1}$, 1979–2008). **(b)** Seasonal averaged rainfall (in mm day$^{-1}$) in PLC experiment with RegCM4 (1982–2008). **(c)** Seasonal averaged rainfall in PLCS experiment (in mm day$^{-1}$, 1982–2008). **(d)** Seasonal averaged rainfall based on IMD data (in mm day$^{-1}$, 1979–2007). **(e)** Seasonal averaged rainfall based on APHRODITE data (in mm day$^{-1}$, 1979–2007). **(f)** Seasonal averaged rainfall only over land in PLC experiment (in mm day$^{-1}$).

Title Page
Abstract
Introduction
Conclusions
References
Tables
Figures
◀◀
▶▶
◀
▶
Back
Close
Full Screen / Esc
Printer-friendly Version
Interactive Discussion

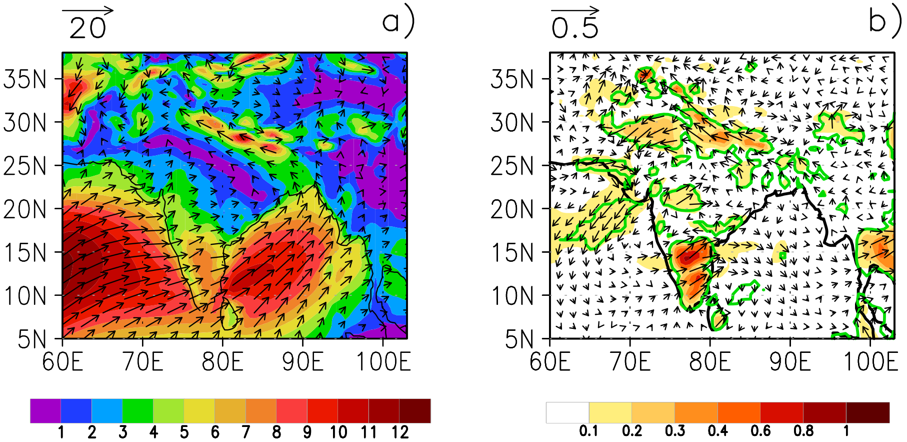

**Figure 5.** Seasonal (JJAS) averaged wind at 10 m (in $\mathrm{m\,s^{-1}}$, 1982–2008). **(a)** Climatological mean (PLC experiment) and **(b)** difference (PLC-HLC). The shaded color depicts magnitude and arrows show the direction. Green contour shows differences significant at 90 % confidence level.

Title Page

Abstract | Introduction

Conclusions | References

Tables | Figures

◀| |▶

◀ ▶

Back | Close

Full Screen / Esc

Printer-friendly Version

Interactive Discussion

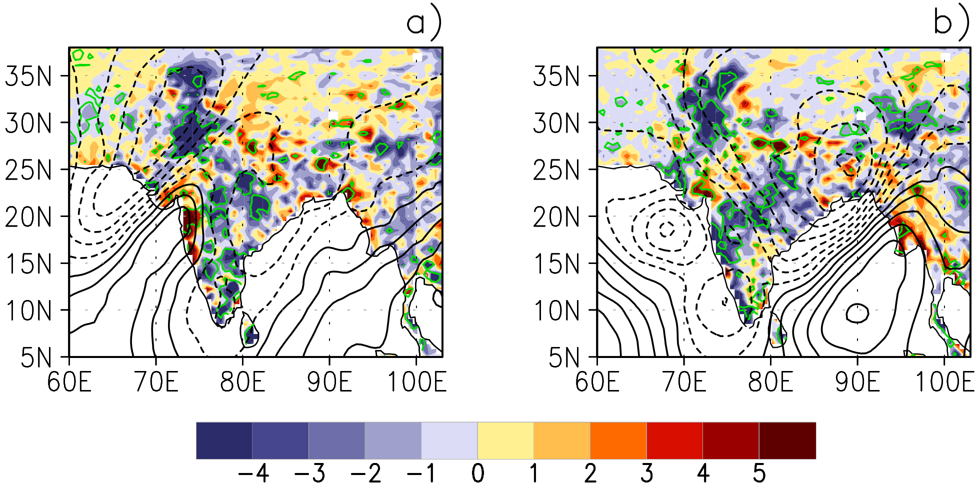

**Figure 6. (a)** Difference (PLC-HLC experiment) in climatological mean seasonal rainfall (in cm, 1982–2008) shown in shaded color. **(b)** Same as in **(a)** but for PLCS-HLCS experiments. Dashed (solid) black contours show the decrease (increase) in velocity potential analog (or the divergent component) of vertically integrated moisture flux $q\boldsymbol{V}$ (from surface–300 hPa). The contour interval is in $1 \times 10^6$ kg s$^{-1}$. Green contour shows differences significant at the 90 % confidence level.

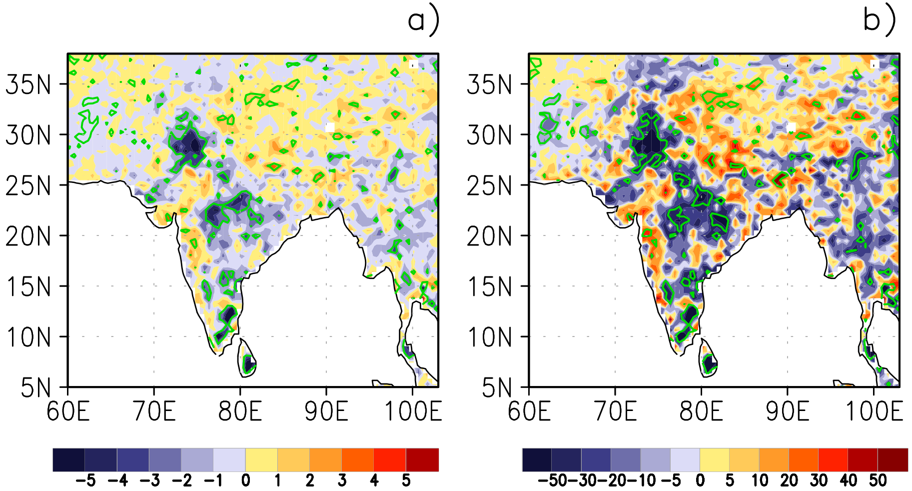

**Figure 7.** Difference (PLC-HLC) in **(a)** number of moderate rainfall events during JJAS and **(b)** total amount of moderate rainfall (in mm day$^{-1}$, 1982–2008). Green contour shows differences significant at the 90 % confidence level.

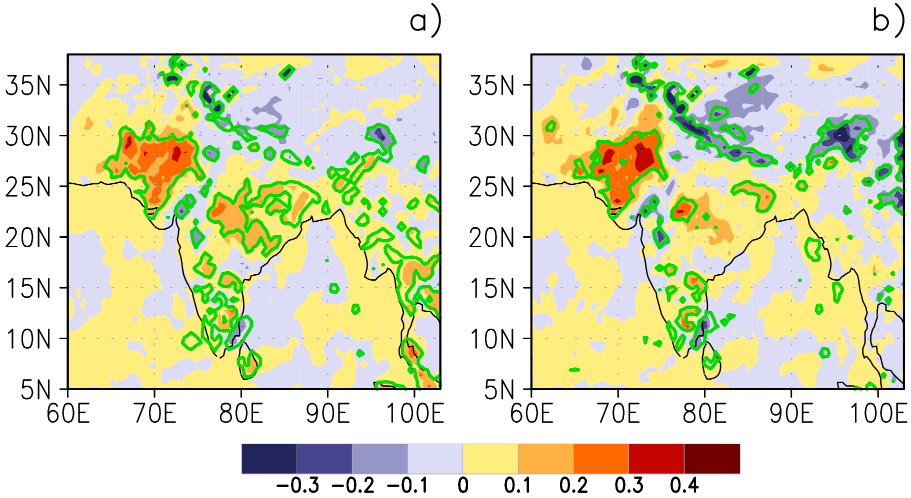

**Figure 8.** Difference (PLC-HLC) in JJAS averaged 2 m air temperature (in °C, 1982–2008), for **(a)** daily mean, and **(b)** daily maximum temperature. Green contour shows significance at 90 % confidence levels.

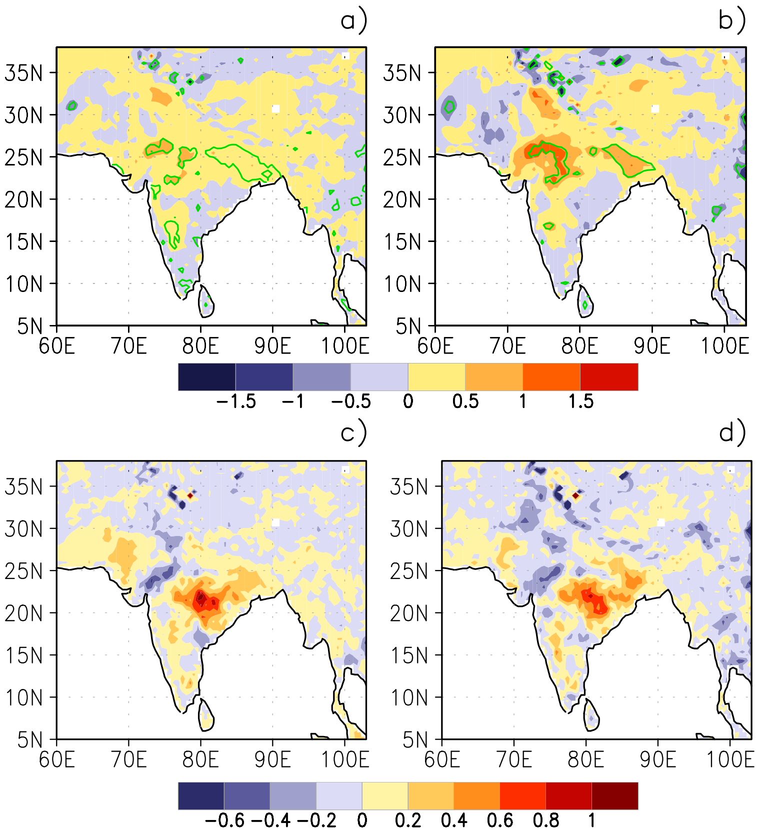

**Figure 9.** Difference (PLC-HLC) in daily variance of 2 m air temperature in JJAS (in °C$^2$, 1982–2008) for **(a)** daily mean, and **(b)** daily maximum temperature. Green contour shows significance at 90 % confidence level. Difference (PLC-HLC) in the 90th percentile of daily 2 m air temperature in JJAS (in °C, 1982–2008), for **(c)** daily mean and **(d)** daily maximum temperature.

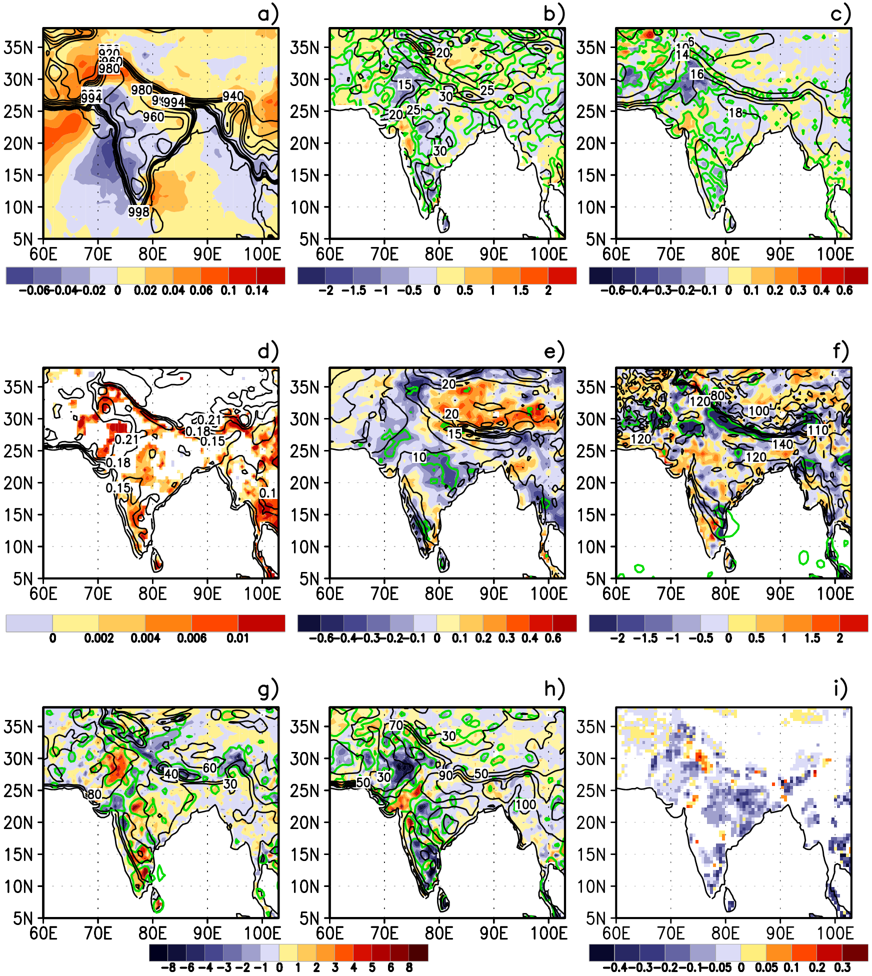
a)
b)
c)
d)
e)
f)
g)
h)
i)
35N
30N
25N
20N
15N
10N
5N
60E
70E
80E
90E
100E
920
960
980
994
980
994
940
960
998
20
15
30
25
20
25
30
16
14
16
18
0.21
0.18
0.15
0.21
0.18
0.15
0.1
20
20
15
10
120
80
100
110
120
140
120
40
60
30
80
70
30
50
30
90
50
100
−0.06 −0.04 −0.02 0 0.02 0.04 0.06 0.1 0.14
−2 −1.5 −1 −0.5 0 0.5 1 1.5 2
−0.6 −0.4 −0.3 −0.2 −0.1 0 0.1 0.2 0.3 0.4 0.6
0 0.002 0.004 0.006 0.01
−0.6 −0.4 −0.3 −0.2 −0.1 0 0.1 0.2 0.3 0.4 0.6
−2 −1.5 −1 −0.5 0 0.5 1 1.5 2
−8 −6 −4 −3 −2 −1 0 1 2 3 4 5 6 8
−0.4 −0.3 −0.2 −0.1 −0.05 0 0.05 0.1 0.2 0.3

**Figure 10.** **(a)** Seasonal (JJAS) averaged surface pressure in PLC experiment (in black contours) and its difference (PLC-HLC) in shaded color (in hPa, 1982–2008). Green contour shows differences significant at 90 % confidence level. **(b–i)** Show similar differences as in **(a)** but for surface soil moisture (0–10 cm, in mm), 2 m specific humidity (in $\mathrm{g\,kg^{-1}}$), surface albedo (unitless), total cloud cover (in %), surface net radiation (in $\mathrm{W\,m^{-2}}$), surface sensible heat flux (in $\mathrm{W\,m^{-2}}$), surface latent heat flux (in $\mathrm{W\,m^{-2}}$), respectively. **(i)** Shows only the difference (PLC-HLC) in sum of transpiration and evaporation of canopy-intercepted water (in $\mathrm{mm\,day^{-1}}$). In **(d)** and **(i)**, only the differences significant at 90 % confidence level are shaded.

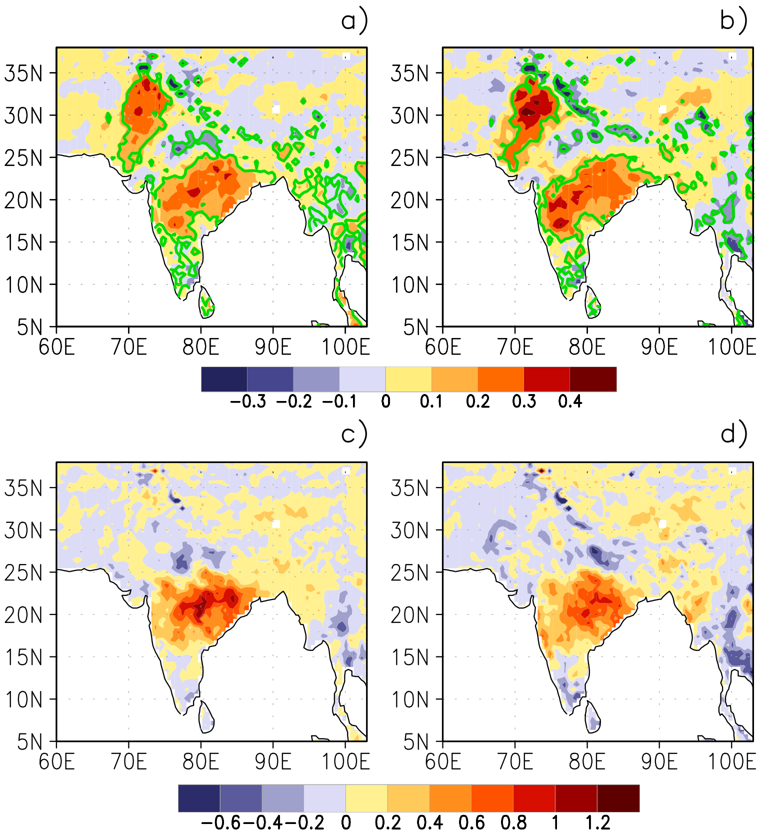

**Figure 11.** Difference (PLCS-HLCS) in seasonal (JJAS) averaged 2 m air temperatures (in °C, 1982–2008) for **(a)** daily mean, and **(b)** daily maximum temperature. Green contour shows differences significant at 90 % confidence level. Difference (PLCS-HLCS) in the 90th percentile of daily 2 m air temperature in JJAS (in °C, 1982–2008), for **(c)** daily mean, and **(d)** daily maximum temperature.

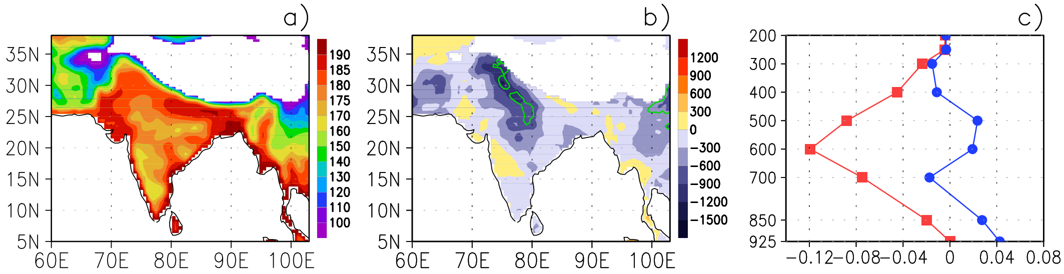

**Figure 12. (a)** Seasonal average (JJAS) of vertically integrated moist static energy (VIMSE, surface-500 hPa) in PLC experiment (in $1 \times 10^4$ kJ kg$^{-1}$, 1982–2008). **(b)** Difference (PLC-HLC) in VIMSE (in kJ kg$^{-1}$, 1982–2008). Green contour shows differences significant at 90 % confidence level. **(c)** Difference (PLC-HLC) in CI averaged moist static energy (MSE, in red) and dry static energy (DSE, in blue) in units of kJ kg$^{-1}$.